

SU(3) altermagnetism: Lattice models, chiral magnons, and flavor-split bands

Pedro M. C nsoli and Matthias Vojt 

*Institut f r Theoretische Physik and W rzburg-Dresden Cluster of Excellence ct.qmat,
Technische Universit t Dresden, 01062 Dresden, Germany*

(Dated: March 1, 2024)

Altermagnetism, a type of magnetic order that combines properties of ferromagnets and antiferromagnets, has generated significant interest recently, in particular due to its potential spintronics applications. Here, we show that altermagnetic states, which typically involve collinear magnetic order of SU(2) spins, can be generalized to higher SU(N) symmetry groups. We construct a two-dimensional Heisenberg model for a three-sublattice SU(3) altermagnet and analyze its excitation spectrum via flavor-wave theory. By deriving a general formula for the chirality of the excitations, we show that the SU(3) altermagnet harbors chiral magnons that are split in energy. We also compute the electronic band structure for a metallic system of the same symmetry and map out the polarization of the resulting flavor-split bands. We conclude by discussing further generalizations.

Altermagnetism represents an unconventional type of magnetic order, beyond standard ferromagnetism or antiferromagnetism, which is currently attracting a lot of attention [1, 2]. Altermagnetic states have vanishing uniform magnetization, but display a variety of properties typically associated with ferromagnets, such as electronic bands which are spin-split in the absence of spin-orbit coupling, and associated macroscopic magneto-transport phenomena. These properties make altermagnets interesting both on fundamental grounds as well as for spintronics applications [2, 3]. Microscopically, the magnetic sublattices of altermagnets are related by symmetry operations other than translation and inversion, giving rise to spin polarization in reciprocal space. A formal description based on a spin-space symmetry classification can be found in Ref. 1. In addition to their special conduction-band properties, altermagnets also feature a nontrivial magnon spectrum: the dispersions of magnons of different chirality split in an anisotropic fashion, again dictated by the underlying spin-space symmetries [4]. The vast majority altermagnetic states discussed to date feature collinear magnetic order of SU(2) moments, experimental examples being RuO₂ [5, 6], MnTe [7], and thin-film Mn₅Si₃ [8]. Extensions to non-collinear spins have been discussed in Refs. 9 and 10.

The purpose of this paper is to generalize the concept of altermagnetism to higher SU(N) symmetry groups. For concreteness, we focus on SU(3) and follow the principle noted above to construct a system with a three-color ground state in which the magnetic sublattices are not related by translation nor inversion, but only by rotation or mirror symmetries. We first consider a Heisenberg-type model on a modified triangular lattice and determine its magnon spectrum using flavor-wave theory. After developing a general approach to compute the magnon chirality, we demonstrate that the SU(3) altermagnet displays chiral magnons, with modes of different chirality split in energy. Including charge carriers, we then consider an SU(3) double-exchange model on the same lattice and determine its electronic band structure. We find that the

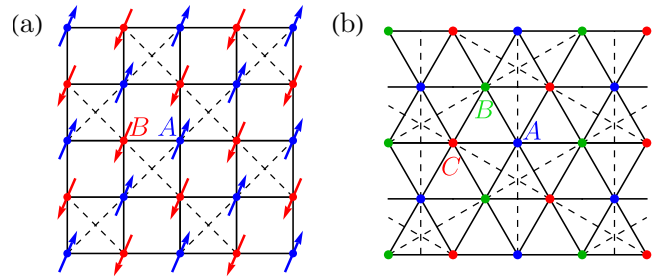


FIG. 1. Lattice structures of altermagnetic Heisenberg models: (a) Checkerboard lattice with collinear SU(2) order; (b) Hexatriangular lattice with three-color SU(3) order. Solid (dashed) lines show couplings J_1 (J_2), respectively.

electronic bands are flavor-split at generic momenta and have crossings dictated by spin-point-group symmetries, consisting of the combination of lattice point-group operations and independent transformations in spin space [1, 11, 12]. For comparison, we perform the same steps for models on a modified square lattice (namely, the checkerboard lattice) with collinear SU(2) spin order, which has appeared as a motif for altermagnetism in another recent paper [13]. In doing so, we demonstrate that our approach reproduces multiple known properties of SU(2) altermagnets. We discuss further generalizations and applications of our ideas.

Heisenberg models of altermagnets. – While altermagnets resemble antiferromagnets in the sense of vanishing total magnetization, they lack those translation and inversion symmetries which would otherwise map the two magnetic sublattices into each other. In real-world compounds, this lack of symmetry is often due to the presence of non-magnetic atoms whose lattice structure spoils the translation and inversion symmetries of the lattice of magnetic atoms. Here we implement this symmetry breaking on a model level. To keep things conceptually simple, we start by constructing Heisenberg-type spin models for insulating altermagnets, and add conduction electrons in a later step. We thus consider SU(N)

Hamiltonians of the form [14–18]

$$\mathcal{H}_S = \frac{1}{2N} \sum_{jj'} \sum_{\alpha, \beta=1}^N J_{jj'} S_j^{\alpha\beta} S_{j'}^{\beta\alpha}, \quad (1)$$

where α, β are $SU(N)$ flavor indices and $J_{jj'}$ is the exchange coupling between sites j and j' . For every j , the symbols $S_j^{\alpha\beta}$ denote generators of the $SU(N)$ algebra in the totally symmetric $(M, 0)$ irreducible representation, which corresponds to a Young tableau with M boxes in a single row. Furthermore, they obey the commutation relations $[S_j^{\beta\alpha}, S_j^{\beta'\alpha'}] = S_j^{\beta\alpha'} \delta_{\alpha\beta'} - S_j^{\beta'\alpha} \delta_{\alpha'\beta}$. Each local state in the representation is uniquely characterized by its eigenvalues with respect to the diagonal generators ($\alpha = \beta$), which have integer eigenvalues $0, \dots, M$ and are subject to the condition $\sum_{\alpha} S_j^{\alpha\alpha} = M$. For $N = 2$, the nondiagonal generators are nothing but the familiar ladder operators S_j^{\pm} , and Eq. (1) becomes $\mathcal{H}_S = \frac{1}{2} \sum_{jj'} J_{jj'} \mathbf{S}_j \cdot \mathbf{S}_{j'}$, with spins $S = M/2$, apart from an irrelevant constant. In the following, we investigate the above models in the semiclassical regime of large M . Results obtained in this manner will be qualitatively valid also for small M provided that the respective magnetic order occurs.

The construction of the altermagnetic models then proceeds in two steps: (i) Start with a simple model which yields the desired type of antiferromagnetic order. (ii) Augment this model with additional couplings that break translation and inversion symmetries between the sublattices so as to turn the ordered phase into an altermagnet.

We demonstrate this procedure first for the $SU(2)$ case in order to connect to previous work. For step (i), we consider spins S placed on each site of a square lattice and interacting via nearest-neighbor antiferromagnetic couplings J_1 . Collinear Néel order divides the system into sublattices A and B. For step (ii), we add second-neighbor couplings J_2 which run along one diagonal for sublattice A and along the other for sublattice B. This results in the checkerboard lattice, Fig. 1(a), with a crystallographic unit cell of two sites and D_4 point-group symmetry. Different magnetic sublattices are related either by mirror operations or by $\pm 90^\circ$ rotations about the center of an elementary square plaquette.

For the $SU(3)$ case, we start in step (i) with a nearest-neighbor model on the triangular lattice, where an antiferromagnetic coupling J_1 leads to three-sublattice three-color order in the ground state [18–20]. In step (ii) we add selected second-neighbor couplings J_2 which run along different directions for the three sublattices, A, B, and C. As shown in Fig. 1(b), the resulting lattice features a three-site unit cell and six inequivalent elementary triangular plaquettes, for which reason we dub it the hexatriangular lattice. The magnetic sublattices are now related by D_3 point-group operations about the center of a filled triangle, namely 120° rotations and reflections

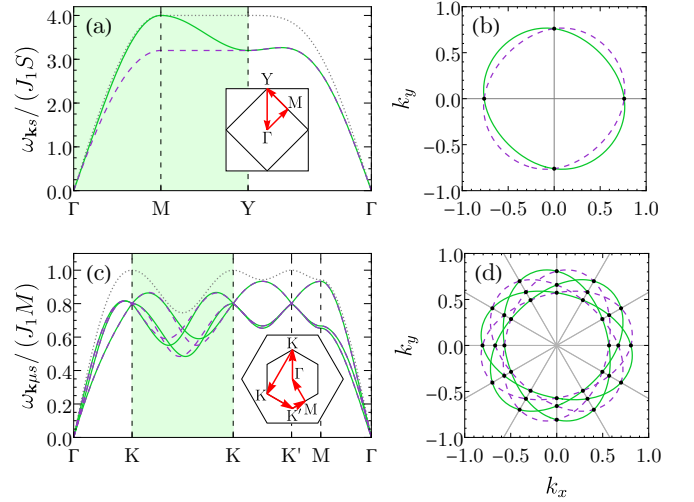


FIG. 2. Magnon dispersions of the (a,b) $SU(2)$ and (c,d) $SU(3)$ Heisenberg altermagnets for $J_2/J_1 = 0.2$. The solid green (dashed purple) bands correspond to modes with positive (negative) chirality. The left panels show the dispersions along paths in momentum space which are indicated in the insets; regions shaded in light green highlight sections where the band splitting is evident, whereas the dotted gray line is the dispersion for $J_2 = 0$. The right panels depict isoenergy contours at (b) $E = 1.8J_1$ and (d) $E = 0.35J_1$.

with respect to dashed lines in Fig. 1(b). Generalizations to higher space dimensions and larger N are clearly possible.

We will now discuss the properties of these Heisenberg models at zero temperature. We will work in a regime where $|J_2|/J_1$ is sufficiently small such that the semiclassical ordered state is unaltered by the presence of J_2 .

Spin waves and flavor waves. – In the $SU(2)$ case, we perform standard linear spin-wave theory as in Ref. 21. To account for the two-sublattice structure, we label sites as $j = (i\mu)$, with i and $\mu = A, B$ being unit-cell and sublattice indices, respectively. Using a Holstein-Primakoff representation in terms of bosons a_i and b_i , such that $S_{iA}^z = S - a_i^\dagger a_i$ and $S_{iB}^z = -S + b_i^\dagger b_i$, we find that the bilinear piece of the Hamiltonian reads

$$\mathcal{H}_S^{(2)} = 4J_1 S \sum_{\mathbf{k}} \Psi_{\mathbf{k}}^\dagger \begin{pmatrix} 1 - 2\eta\Gamma_{\mathbf{k}1} & \gamma_{\mathbf{k}} \\ \gamma_{\mathbf{k}} & 1 - 2\eta\Gamma_{\mathbf{k}2} \end{pmatrix} \Psi_{\mathbf{k}} \quad (2)$$

with $\Psi_{\mathbf{k}}^\dagger = (a_{\mathbf{k}}^\dagger, b_{-\mathbf{k}})$, $\eta = J_2/(4J_1)$, and form factors $\gamma_{\mathbf{k}} = (\cos k_x + \cos k_y)/2$ and $\Gamma_{\mathbf{k}1,2} = 1 - \cos(k_x \pm k_y)$. Diagonalizing $\mathcal{H}_S^{(2)}$ by a Bogoliubov transformation yields the spectrum [21]

$$\frac{\omega_{\mathbf{k}\pm}}{4J_1 S} = \sqrt{[1 - \eta(\Gamma_{\mathbf{k}1} + \Gamma_{\mathbf{k}2})]^2 - \gamma_{\mathbf{k}}^2 \pm \eta(\Gamma_{\mathbf{k}2} - \Gamma_{\mathbf{k}1})}, \quad (3)$$

For $J_2 = 0$, we have two degenerate spin-wave modes, $\omega_{\mathbf{k}+} = \omega_{\mathbf{k}-}$, which split for any $J_2 \neq 0$. As illustrated in

Fig. 2(a,b), the splitting occurs for all momenta except along the lines $k_x = 0$ and $k_y = 0$, where the degeneracy is enforced by the fact that both the Hamiltonian and the magnetic ground state are invariant under a transformation that combines spin inversion with a mirror operation that exchanges sublattices A and B [1]. We will show below that the s index in $\omega_{\mathbf{k}s}$ is directly related to the chirality of the magnon.

For the SU(3) model, we investigate the magnetic excitations via linear flavor-wave theory, a method formally based on a $1/M$ expansion [16–20, 22, 23]. We start with the large- M ground state $|\psi\rangle = \otimes_{i\mu} |\mu\rangle_{i\mu}$, where $\mu = A, B, C$ is an index for both sublattice and color, and $S_{i\mu}^{\alpha\alpha} |\mu\rangle_{i\mu} = \delta_{\alpha\mu} M |\mu\rangle_{i\mu}$. We introduce two flavors of Holstein-Primakoff bosons $a_{i\mu\alpha}$ at every site $(i\mu)$ with $\alpha \neq \mu$ which obey $a_{i\mu\alpha} |\psi\rangle = 0$, while the $a_{i\mu\alpha}^\dagger$ change the eigenvalues of a given state with respect to the diagonal operators $S_{i\mu}^{\alpha\alpha}$ and $S_{i\mu}^{\mu\mu}$ by $+1$ and -1 , respectively. By identifying $\{A, B, C\} \equiv \{1, 2, 3\} \bmod 3$, the bilinear piece of the Hamiltonian reads (see Ref. 24 for the derivation)

$$\frac{\mathcal{H}_S^{(2)}}{J_1 M} = \sum_{\mathbf{k}\mu} \Psi_{\mathbf{k}\mu}^\dagger \begin{pmatrix} 1 - 2\tilde{\eta}\tilde{\Gamma}_{\mathbf{k},\mu+1} & \tilde{\gamma}_{\mathbf{k}} \\ \tilde{\gamma}_{\mathbf{k}}^* & 1 - 2\tilde{\eta}\tilde{\Gamma}_{\mathbf{k},\mu-1} \end{pmatrix} \Psi_{\mathbf{k}\mu} \quad (4)$$

with $\Psi_{\mathbf{k}\mu}^\dagger = \begin{pmatrix} a_{\mathbf{k},\mu+1,\mu-1}^\dagger & a_{-\mathbf{k},\mu-1,\mu+1} \end{pmatrix}$ and $\tilde{\eta} = J_2/(3J_1)$. The form factors here are $\tilde{\gamma}_{\mathbf{k}} = \frac{1}{3} \sum_{\delta_1} e^{i\mathbf{k} \cdot \delta_1}$ and $\tilde{\Gamma}_{\mathbf{k}\mu} = 1 - \cos(\mathbf{k} \cdot \delta_{2\mu})$, where δ_1 represents the three vectors from a site $(i\mu)$ to its nearest neighbors on sublattice $\mu+1$, and $\delta_{2\mu}$ connects second neighbors on the same sublattice μ . Equation (4) is a 6×6 block-diagonal Hamiltonian with three 2×2 blocks, each labeled by the sublattice μ that is *not* affected by the generated combinations of bosonic operators. Importantly, this is not a special feature of the hexatriangular lattice, and has been recognized as a consequence of SU(N) symmetry in an early SU(4) flavor-wave study [17]. The magnon dispersion follows from diagonalization and reads

$$\frac{\omega_{\mathbf{k}\mu\pm}}{J_1 M} = \sqrt{\left[1 - \tilde{\eta} \left(\tilde{\Gamma}_{\mathbf{k},\mu-1} + \tilde{\Gamma}_{\mathbf{k},\mu+1}\right)\right]^2 - |\tilde{\gamma}_{\mathbf{k}}|^2} \pm \tilde{\eta} \left(\tilde{\Gamma}_{\mathbf{k},\mu-1} - \tilde{\Gamma}_{\mathbf{k},\mu+1}\right) \quad (5)$$

For $J_2 = 0$ this expression agrees with earlier results [18, 20] and yields a sixfold degeneracy in the reduced Brillouin zone. However, as shown in Fig. 2(c,d), a $J_2 \neq 0$ leads to the complete splitting of the magnon modes throughout most of reciprocal space. Exceptions occur along high-symmetry lines with polar angle $\phi_{\mathbf{k}} = n\pi/6$ and the boundaries of the Brillouin zone, where partial degeneracies between modes of opposite s are protected by spin-space symmetries [24].

Magnon chirality. – Consider an excited state containing magnons of a single momentum and species, but

which is otherwise arbitrary. For the SU(2) model above, this would be $|\phi_{\mathbf{k}s}\rangle = \sum_{n=0}^{\infty} c_n |n_{\mathbf{k}s}\rangle$, where $|n_{\mathbf{k}s}\rangle$ denotes a state with n magnons of energy $\omega_{\mathbf{k}s}$. We define the chirality κ_s of the corresponding SU(2) magnon mode as the sense of precession (as a function of time) of an individual spin around its classical axis, $\hat{\mathbf{e}}_3$, in the state $|\phi_{\mathbf{k}s}\rangle$:

$$\kappa_s = \text{sgn} \left\{ \left[\langle \mathbf{S}_{iA}(t) \rangle \times \frac{d}{dt} \langle \mathbf{S}_{iA}(t) \rangle \right] \cdot \hat{\mathbf{e}}_3 \right\}. \quad (6)$$

Here, the choice of the site (iA) is arbitrary and $\mathbf{S}_{iA}(t) = e^{i\mathcal{H}_S^{(2)}t} \mathbf{S}_{iA} e^{-i\mathcal{H}_S^{(2)}t}$. Using the eigenstates of Eq. (2), a straightforward calculation [24] yields

$$\kappa_s = -s, \quad (7)$$

provided that $\xi = \sum_{n=0}^{\infty} \sqrt{n+1} c_n^* c_{n+1} \neq 0$; otherwise, $\kappa_s = 0$. The latter case arises, for instance, when $|\phi_{\mathbf{k}s}\rangle$ has a definite number of magnons, $c_n = \delta_{nm} c_m$, and uncertainty relations prevent the determination of the phase of the precessive motion [25]. Excluding the possibility $\kappa_s = 0$, we can assign a definite chirality (7) to each magnon mode. When $J_2 \neq 0$, the energies $\omega_{\mathbf{k}s}$ (3) of modes with different chiralities κ_s split, as expected for an SU(2) altermagnet [4]. For completeness, we note that, for sites on the B sublattice, the quantity κ_s defined analogously to Eq. (6) would obey $\kappa_s = +s$, reflecting the fact that the spins on the two sublattices precess in phase but with opposite classical ordering directions.

In the SU(3) case, the block-diagonal structure of Eq. (4) implies that each magnon mode only affects two of the three magnetic sublattices, so that spin dynamics is generated exclusively by an SU(2) subalgebra of SU(3) [24]. It allows us to adopt essentially the same definition of chirality as in Eq. (6), which yields $\kappa_s = -s$ for modes with dispersion $\omega_{\mathbf{k}\mu s}$ [24]. Hence, we arrive at two key results of the paper: (i) the magnon modes of the SU(3) hexatriangular model have definite chiralities and (ii) modes with different chiralities split in energy when $J_2 \neq 0$, exactly as in the SU(2) altermagnet.

Electronic band structure. – We now extend our considerations to band-electron properties in the presence of altermagnetic order. To this end, we utilize two-band lattice models built by locally coupling magnetic moments subject to the exchange interactions discussed above to conduction electrons that hop on the same lattice. We moreover restrict the hopping amplitudes $t_{jj'}$ to first- and second-neighbor sites and require that they obey the same spatial symmetries as $J_{jj'}$. The full Hamiltonian then reads $\mathcal{H} = \mathcal{H}_S + \mathcal{H}_e$ with

$$\mathcal{H}_e = - \sum_{jj'} t_{jj'} c_{j\alpha}^\dagger c_{j'\alpha} - \frac{K}{M} \sum_j \sum_{n=1}^{N^2-1} S_j^n c_{j\alpha}^\dagger \tau_{\alpha\beta}^n c_{j\beta} \quad (8)$$

representing the SU(N) generalization of a standard double-exchange [26, 27] or Kondo-lattice [28, 29] Hamiltonian. We assume that the conduction electrons transform under the fundamental representation of SU(N).

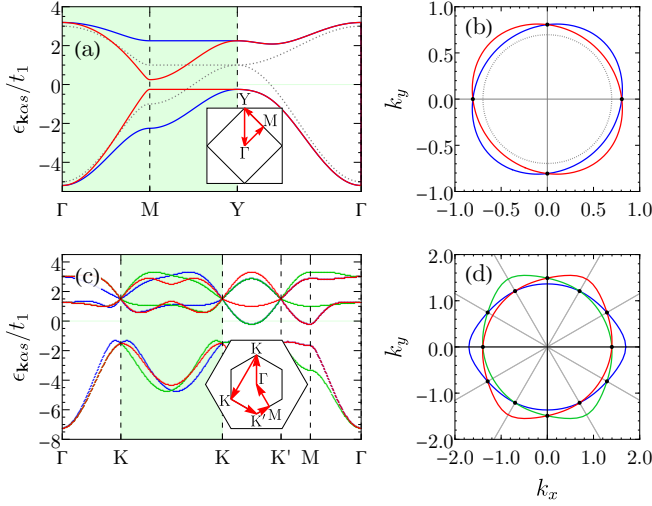


FIG. 3. Band structure of the (a,b) SU(2) and (c,d) SU(3) double-exchange models for parameters $(t_2, K) = (0.5, 5) t_1$ and $(t_2, K) = (0.5, 6.0) t_1$, respectively. Different bands are colored according to their spin or flavor. In the left panels, the shaded green regions indicate the sections of the paths through the Brillouin zones without any degeneracies. The dotted gray lines in (a) and (b) indicate the unsplit bands for $K = 0$. The right panels show isoenergy contours for (b) $E = -4.3t_1$ and (d) $E = -3.7t_1$.

The corresponding generators τ^n are then one-half of the Pauli and Gell-Mann matrices for $N = 2$ and 3, respectively. Meanwhile, the S_j^n denote the $N^2 - 1$ independent generators of the SU(N) algebra in its $(M, 0)$ totally symmetric irreducible representation. $(N - 1)$ of these are diagonal and given by linear combinations of the $S_j^{\alpha\alpha}$. The remaining $N(N - 1)$ nondiagonal generators can be combined to form the raising and lowering operators $S_j^{\alpha\beta}$ with $\alpha \neq \beta$ [24].

We assume that the local moments S_j display long-range altermagnetic order, with a magnetic unit cell of N sites. We treat the model in Eq. (8) by employing a semiclassical approximation in which each S_j^n is replaced by its expectation value with respect to the $M \rightarrow \infty$ ground state $|\psi\rangle$, such that the electrons move in a modulated effective magnetic field $h_j^n = \langle \psi | S_j^n | \psi \rangle$, leading to N^2 electronic bands in the reduced Brillouin zone. When the effective field is invariant under transformations generated by the $(N - 1)$ diagonal generators of the SU(N) algebra, as is the case for collinear SU(2) and three-color SU(3) order, the Bloch eigenstates possess definite flavor α , i.e., \mathcal{H}_e is flavor-diagonal and splits into N separate $N \times N$ blocks.

In the SU(2) checkerboard model, h_j^n takes the form of a staggered Néel field, and the diagonalization of the

hopping problem yields the band structure

$$\epsilon_{\mathbf{k}\alpha\pm} = -2t_2 \cos k_x \cos k_y \pm \sqrt{[2t_2 \sin k_x \sin k_y + (-1)^\alpha K/4]^2 + (4t_1\gamma_{\mathbf{k}})^2}. \quad (9)$$

Thus, each pair of bands $\epsilon_{\mathbf{k}\alpha s}$ with opposite spin α splits once K and t_2 are both nonzero [see Fig. 3(a,b)]. This spin splitting furthermore displays a d -wave symmetry, as required by the spin-space symmetries mentioned above and observed in various d -wave altermagnetic systems [1].

For the SU(3) model, we determine the dispersion by diagonalizing each 3×3 block in \mathcal{H}_e numerically. Similarly to the SU(2) case, we find three different sets of flavor-degenerate bands when either $t_2 = 0$ or $K = 0$, since the system has (in both situations) a three-site unit cell. However, as illustrated in Fig. 3(c,d), nonzero t_2 and K allows the complete splitting of the nine bands. Partial degeneracies occur along high-symmetry lines and are once more protected by spin point-group symmetries, which are presented in detail in the supplement [24].

Conclusion. – We have shown that the concept of SU(2) altermagnetism can be generalized to higher SU(N) symmetry groups. Specifically, we constructed models of SU(3) altermagnetism with three-color order that feature chiral magnons split in energy and flavor-split electronic bands. We also derived a general formula for the magnon chirality, applicable for both SU(2) and SU(3) cases.

While finding SU(N)-symmetric settings with $N > 2$ in solids may be challenging, the models proposed here can potentially be realized using cold-atom systems. Here, the SU(N) degree of freedom is represented by different hyperfine states of alkaline-earth atoms [30–34] and couplings can be engineered to be SU(N)-symmetric [32]. In fact, Ref. 13 proposed a cold-atom realization of an SU(2) altermagnetic Hubbard model which, in the strong coupling-limit, reduces to the checkerboard-lattice Heisenberg model in Eq. (1). Since triangular lattices can be engineered in cold-atom settings as well [35], we believe that implementing the SU(3) models proposed in this paper is within reach.

It can be expected that the SU(3) altermagnetic models presented here will display transport characteristics known from SU(2) altermagnets, such as an anomalous Hall effect [36, 37], an anomalous Nernst effect as well as further spin caloritronics phenomena originally found for ferromagnets [2]. A detailed study of transport properties of altermagnets with higher symmetry groups is left for future work.

There are various straightforward generalizations to the constructions principles proposed here. For instance, four-sublattice four-color order can be realized for SU(4) exchange models on the square lattice [38, 39], and an altermagnet can be obtained by adding suitable further-neighbor couplings. Alternatively, lattices with larger

crystallographic unit cells are natural starting points for $\mathbf{Q} = 0$ altermagnetic order, such as kagome and hyperkagome lattices for SU(3) and the pyrochlore lattice for SU(4). Investigations in these directions are under way.

We thank S.-W. Cheong for helpful discussions. Financial support from the DFG through SFB 1143 (project-id 247310070) and the Würzburg-Dresden Cluster of Excellence on Complexity and Topology in Quantum Matter – *ct.qmat* (EXC 2147, project-id 390858490) is gratefully acknowledged.

-
- [1] L. Šmejkal, J. Sinova, and T. Jungwirth, *Phys. Rev. X* **12**, 031042 (2022).
 - [2] L. Šmejkal, J. Sinova, and T. Jungwirth, *Phys. Rev. X* **12**, 040501 (2022).
 - [3] R. González-Hernández, L. Šmejkal, K. Vyborny, Y. Yahagi, J. Sinova, T. Jungwirth, and J. Zelezny, *Phys. Rev. Lett.* **126**, 127701 (2021).
 - [4] L. Šmejkal, A. Marmodoro, K.-H. Ahn, R. González-Hernández, I. Turek, S. Mankovsky, H. Ebert, S. W. D'Souza, O. Šipr, J. Sinova, and T. Jungwirth, *Phys. Rev. Lett.* **131**, 256703 (2023).
 - [5] Z. Feng *et al.*, *Nat. Electron.* **5**, 735 (2022).
 - [6] T. Tschirner *et al.*, *APL Mater.* **11**, 101103 (2023).
 - [7] R. D. Gonzalez Betancourt *et al.*, *Phys. Rev. Lett.* **130**, 036702 (2023).
 - [8] H. Reichlová *et al.*, arXiv:2012.15651.
 - [9] S.-W. Cheong, *npj Quant. Mater.* **5**, 37 (2020).
 - [10] S.-W. Cheong and F.-T. Huang, *npj Quant. Mater.* **9**, 13 (2024).
 - [11] D. M. Litvin and W. Opechowski, *Physica* **76**, 538 (1974).
 - [12] D. M. Litvin, *Acta Cryst.* **A33**, 279 (1977).
 - [13] P. Das, V. Leeb, J. Knolle, and M. Knap, arXiv:2312.10151.
 - [14] I. Affleck, *Phys. Rev. Lett.* **54**, 966 (1985).
 - [15] N. Read and S. Sachdev, *Nucl. Phys. B* **316**, 609 (1989).
 - [16] N. Papanicolaou, *Nucl. Phys. B* **305**, 367 (1988).
 - [17] A. Joshi, M. Ma, F. Mila, D. N. Shi, and F. C. Zhang, *Phys. Rev. B* **60**, 6584 (1999).
 - [18] B. Bauer, P. Corboz, A. M. Läuchli, L. Messio, K. Penc, M. Troyer, and F. Mila, *Phys. Rev. B* **85**, 125116 (2012).
 - [19] A. Läuchli, F. Mila, and K. Penc, *Phys. Rev. Lett.* **97**, 087205 (2006).
 - [20] H. Tsunetsugu and M. Arikawa, *J. Phys. Soc. Jpn.* **75**, 083701 (2006).
 - [21] B. Canals, *Phys. Rev. B* **65**, 184408 (2002).
 - [22] N. Papanicolaou, *Nucl. Phys. B* **240**, 281 (1984).
 - [23] T. Sommer, M. Vojta, and K. W. Becker, *Eur. Phys. J. B* **23**, 329 (2001).
 - [24] See supplemental material for details of the spin-wave and flavor-wave calculations, a derivation of the magnon-chirality formula, as well as an analysis of spin point-group symmetries and their effect on the electronic bands of the Kondo-lattice models. The supplement also includes Refs. 40 and 41.
 - [25] P. Carruthers and M. M. Nieto, *Rev. Mod. Phys.* **40**, 411 (1968).
 - [26] P. W. Anderson and H. Hasegawa, *Phys. Rev.* **100**, 675 (1955).
 - [27] P.-G. de Gennes, *Phys. Rev.* **118**, 141 (1960).
 - [28] A. C. Hewson, *The Kondo Problem to Heavy Fermions*, Cambridge University Press, Cambridge (1997).
 - [29] O. Parcollet, A. Georges, G. Kotliar, and A. Sengupta, *Phys. Rev. B* **58**, 3794 (1998).
 - [30] A. V. Gorshkov, M. Hermele, V. Gurarie, C. Xu, P. S. Julienne, J. Ye, P. Zoller, E. Demler, M. D. Lukin, and A. M. Rey, *Nat. Phys.* **6**, 289 (2010).
 - [31] G. Pagano, M. Mancini, G. Cappellini, P. Lombardi, F. Schäfer, H. Hu, X.-J. Liu, J. Catani, C. Sias, M. Inguscio, and L. Fallani, *Nat. Phys.* **10**, 198 (2014).
 - [32] X. Zhang, M. Bishof, S. L. Bromley, C. V. Kraus, M. S. Safranov, P. Zoller, A. M. Rey, and J. Ye, *Science* **345**, 1467 (2014).
 - [33] C. Hofrichter, L. Riegger, F. Scazza, M. Höfer, D. R. Fernandes, I. Bloch, and S. Fölling, *Phys. Rev. X* **6**, 021030 (2016).
 - [34] M. A. Cazalilla and A. M. Rey, *Rep. Prog. Phys.* **77**, 124401 (2014).
 - [35] J. Mongkolkeha, L. Liu, D. Garwood, J. Yang, and P. Schauss, *Phys. Rev. A* **108**, L061301 (2023).
 - [36] N. Nagaosa, J. Sinova, S. Onoda, A. H. MacDonald, and N. P. Ong, *Rev. Mod. Phys.* **82**, 1539 (2010).
 - [37] L. Šmejkal, R. González-Hernández, T. Jungwirth, and J. Sinova, *Sci. Adv.* **6**, eaaz8809 (2020).
 - [38] K. Harada, N. Kawashima, and M. Troyer, *Phys. Rev. Lett.* **90**, 117203 (2003).
 - [39] P. Corboz, A. M. Läuchli, K. Penc, M. Troyer, and F. Mila, *Phys. Rev. Lett.* **107**, 215301 (2011).
 - [40] A. Zee, *Group Theory in a Nutshell for Physicists*, Princeton University Press (2016).
 - [41] T. A. Tóth, A. M. Läuchli, F. Mila, and K. Penc, *Phys. Rev. Lett.* **105**, 265301 (2010).

Supplemental material for: **SU(3) altermagnetism: Lattice models, chiral magnons, and flavor-split bands**

Pedro M. Cônsoli and Matthias Vojta
*Institut für Theoretische Physik and Würzburg-Dresden Cluster of Excellence ct.qmat,
 Technische Universität Dresden, 01062 Dresden, Germany*
 (Dated: March 1, 2024)

S1. SU(2) LOCAL-MOMENT ALTERMAGNET ON THE CHECKERBOARD LATTICE

In this section, we compute the spectrum, discuss certain symmetries, and derive the chirality of the magnon modes of the SU(2) Heisenberg model considered in the main text. The Hamiltonian

$$\mathcal{H} = J_1 \sum_{\langle i\mu, j\nu \rangle} \mathbf{S}_{i\mu} \cdot \mathbf{S}_{j\nu} + J_2 \sum_{\langle\langle i\mu, j\mu \rangle\rangle} \mathbf{S}_{i\mu} \cdot \mathbf{S}_{j\mu} \quad (\text{S1})$$

has spins S placed on the sites $(i\mu)$ of a checkerboard lattice, with i and $\mu = A, B$ being unit-cell and sublattice indices. $J_1, J_2 > 0$ correspond to the solid and dashed couplings in Fig. 1(a) of the main paper. We shall treat the Hamiltonian within standard spin-wave theory, using the Holstein-Primakoff representation.

A. Spin-wave theory

Assuming two-sublattice Néel-type order and introducing Holstein-Primakoff bosons a_i and b_i for the sublattices A and B , respectively, we expand the Hamiltonian as a power series in $1/S$, $\mathcal{H} = \sum_{n=0}^{\infty} S^{2-n/2} \mathcal{H}^{(n)}$. By truncating the series at order $n = 2$, we obtain the linear spin-wave Hamiltonian

$$\mathcal{H}_{\text{LSW}} = N_s S (S + 1) (J_2 - 2J_1) + 4J_1 S \sum_{\mathbf{k}} \left[(1 - 2\eta\Gamma_{\mathbf{k}1}) a_{\mathbf{k}}^\dagger a_{\mathbf{k}} + (1 - 2\eta\Gamma_{\mathbf{k}2}) b_{-\mathbf{k}} b_{-\mathbf{k}}^\dagger + (\gamma_{\mathbf{k}} a_{\mathbf{k}}^\dagger b_{-\mathbf{k}}^\dagger + \text{h.c.}) \right]. \quad (\text{S2})$$

Here, $N_s = 2N_c$ denotes the total number of lattice sites, and Fourier-transformed operators were introduced according to $a_i = N_c^{-1/2} \sum_{\mathbf{k}} e^{i\mathbf{k} \cdot \mathbf{r}_{iA}} a_{\mathbf{k}}$. The constant $\eta = J_2/(4J_1)$ is defined as in the main text, as are the functions $\gamma_{\mathbf{k}}$ and $\Gamma_{\mathbf{k}\mu}$. Thus, the bilinear piece of Eq. (S2) is identical to Eq. (2) of the main text.

After diagonalization via a Bogoliubov transformation, the linear spin-wave Hamiltonian takes the form

$$\mathcal{H}_{\text{LSW}} = NS (S + 1) (J_2 - 2J_1) + \sum_{\mathbf{k}} \sum_{s=\pm} \omega_{\mathbf{k}s} \left(\alpha_{\mathbf{k}s}^\dagger \alpha_{\mathbf{k}s} + \frac{1}{2} \right) \quad (\text{S3})$$

with $\omega_{\mathbf{k}\pm}$ as specified in Eq. (3) of the main text. The magnon eigenmodes are given by

$$\begin{pmatrix} \alpha_{\mathbf{k},+} \\ \alpha_{-\mathbf{k},-}^\dagger \end{pmatrix} = \begin{pmatrix} u_{\mathbf{k}} & -v_{\mathbf{k}} \\ -v_{\mathbf{k}} & u_{\mathbf{k}} \end{pmatrix} \begin{pmatrix} a_{\mathbf{k}} \\ b_{-\mathbf{k}}^\dagger \end{pmatrix}, \quad (\text{S4})$$

with Bogoliubov coefficients

$$u_{\mathbf{k}} = \sqrt{\frac{4J_1 - J_2 (\Gamma_{\mathbf{k}1} + \Gamma_{\mathbf{k}2})}{(\omega_{\mathbf{k}+} + \omega_{\mathbf{k}-})/S}} + \frac{1}{2}, \quad v_{\mathbf{k}} = -\sqrt{\frac{4J_1 - J_2 (\Gamma_{\mathbf{k}1} + \Gamma_{\mathbf{k}2})}{(\omega_{\mathbf{k}+} + \omega_{\mathbf{k}-})/S}} - \frac{1}{2}. \quad (\text{S5})$$

The ground state $|0\rangle$ of Eq. (S3) satisfies $\alpha_{\mathbf{k}s} |0\rangle = 0$. At the Goldstone wave vector $\mathbf{k} = \mathbf{0}$, both of these coefficients diverge as $(\omega_{\mathbf{k}+} + \omega_{\mathbf{k}-})^{-1/2} \sim \omega_{\mathbf{k}s}^{-1/2}$ for either s . Hence, the products $u_{\mathbf{k}}^2 \omega_{\mathbf{k}s}$ and $v_{\mathbf{k}}^2 \omega_{\mathbf{k}s}$ are always finite and strictly positive. We will invoke this property in the derivation of the magnon chirality in Section S1 B.

B. Magnon chirality

Apart from having different spatial content, the two excitations $\alpha_{\mathbf{k},+}$ and $\alpha_{\mathbf{k},-}$, specified by Eq. (S4), also differ in the dynamical behavior they generate. To see this, consider a state

$$|\phi_{\mathbf{k}s}\rangle = \sum_{n=0}^{\infty} c_n |n_{\mathbf{k}s}\rangle = \sum_{n=0}^{\infty} \frac{c_n}{\sqrt{n!}} \left(\alpha_{\mathbf{k}s}^\dagger \right)^n |0\rangle \quad (\text{S6})$$

with arbitrary complex coefficients c_n . Working in the Heisenberg picture, we now investigate the time evolution of

$$\langle \mathbf{S}_{iA}(t) \rangle = \text{Re} [\langle S_{iA}^+(t) \rangle (\hat{\mathbf{x}} - i\hat{\mathbf{y}})] + \langle S_{iA}^z(t) \rangle \hat{\mathbf{z}}, \quad (\text{S7})$$

where $\langle \dots \rangle = \langle \phi_{\mathbf{k}s} | \dots | \phi_{\mathbf{k}s} \rangle$. The first expectation value in Eq. (S7) is evaluated as follows:

$$\begin{aligned} \langle S_{iA}^+(t) \rangle &\approx \sqrt{\frac{2S}{N_c}} \sum_{m,n} c_m^* c_n \sum_{\mathbf{q}} e^{i\mathbf{q} \cdot \mathbf{r}_{iA}} \langle m_{\mathbf{k}s} | u_{\mathbf{q}} \alpha_{\mathbf{q}+}(t) + v_{\mathbf{q}} \alpha_{-\mathbf{q},-}^\dagger(t) | n_{\mathbf{k}s} \rangle \\ &= \sqrt{\frac{2S}{N_c}} \sum_{m,n} c_m^* c_n \left[\delta_{s+} \delta_{n,m+1} \sqrt{n} u_{\mathbf{k}} e^{i(\mathbf{k} \cdot \mathbf{r}_{iA} - \omega_{\mathbf{k}+} t)} + \delta_{s-} \delta_{m,n+1} \sqrt{n+1} v_{-\mathbf{k}} e^{-i(\mathbf{k} \cdot \mathbf{r}_{iA} - \omega_{-\mathbf{k},-} t)} \right] \\ &= \sqrt{\frac{2S}{N_c}} e^{si(\mathbf{k} \cdot \mathbf{r}_{iA} - \omega_{\mathbf{k}s} t)} \left[\delta_{s+} u_{\mathbf{k}} \left(\sum_{m=0}^{\infty} \sqrt{m+1} c_m^* c_{m+1} \right) + \delta_{s-} v_{\mathbf{k}} \left(\sum_{n=0}^{\infty} \sqrt{n+1} c_{n+1}^* c_n \right) \right] \\ &= \sqrt{\frac{2S}{N_c}} |\xi| e^{si(\mathbf{k} \cdot \mathbf{r}_{iA} - \omega_{\mathbf{k}s} t + \arg \xi)} (\delta_{s+} u_{\mathbf{k}} + \delta_{s-} v_{\mathbf{k}}). \end{aligned} \quad (\text{S8})$$

In the last step, we used the fact that $v_{\mathbf{k}}$ and $\omega_{\mathbf{k}-}$ are even in \mathbf{k} and defined $\xi(\{c_n\}) = \sum_{n=0}^{\infty} \sqrt{n+1} c_n^* c_{n+1}$. Similarly,

$$\begin{aligned} \langle S_{iA}^z(t) \rangle &= \langle S - a_i^\dagger(t) a_i(t) \rangle = S - \frac{1}{N_c} \sum_{\mathbf{p}, \mathbf{q}} e^{i(\mathbf{p}-\mathbf{q}) \cdot \mathbf{r}_{iA}} \langle a_{\mathbf{q}}^\dagger(t) a_{\mathbf{p}}(t) \rangle \\ &= S - \frac{1}{N_c} \sum_{m,n} c_m^* c_n \sum_{\mathbf{p}, \mathbf{q}} e^{i(\mathbf{p}-\mathbf{q}) \cdot \mathbf{r}_{iA}} \langle m_{\mathbf{k}s} | u_{\mathbf{q}} u_{\mathbf{p}} \alpha_{\mathbf{q}+}^\dagger(t) \alpha_{\mathbf{p}+}(t) + v_{\mathbf{q}} v_{\mathbf{p}} \alpha_{-\mathbf{q},-}^\dagger(t) \alpha_{-\mathbf{p},-}^\dagger(t) | n_{\mathbf{k}s} \rangle \\ &= S - \frac{1}{N_c} \sum_{m,n} c_m^* c_n \sum_{\mathbf{p}, \mathbf{q}} \delta_{\mathbf{p}, \mathbf{q}} \delta_{mn} [\delta_{s+} \delta_{\mathbf{p}, \mathbf{k}} u_{\mathbf{k}}^2 n + v_{\mathbf{p}}^2 (1 + \delta_{s-} \delta_{\mathbf{p}, -\mathbf{k}} n)] \\ &= m - \frac{\zeta}{N_c} (\delta_{s+} u_{\mathbf{k}}^2 + \delta_{s-} v_{\mathbf{k}}^2). \end{aligned} \quad (\text{S9})$$

Here, we have identified the staggered magnetization in the ground state,

$$m = \frac{1}{N_c} \sum_{i\mu} (-1)^\mu \langle 0 | S_{i\mu}^z | 0 \rangle = S - \frac{1}{N_c} \sum_{\mathbf{k}} v_{\mathbf{k}}^2, \quad (\text{S10})$$

and defined $\zeta(\{c_n\}) = \sum_{n=0}^{\infty} |c_n|^2 n$. The latter clearly vanishes when $|\phi_{\mathbf{k}s}\rangle = |0\rangle$, such that we recover $\langle S_{iA}^z(t) \rangle = m$.

After substituting the previous results back into Eq. (S7), one obtains

$$\langle \mathbf{S}_{iA}(t) \rangle = \sqrt{\frac{2S}{N_c}} |\xi| \text{Re } \boldsymbol{\sigma}_{\mathbf{k}s}(t) + \left[m - \frac{\zeta}{N_c} (\delta_{s+} u_{\mathbf{k}}^2 + \delta_{s-} v_{\mathbf{k}}^2) \right] \hat{\mathbf{z}}, \quad (\text{S11})$$

where

$$\boldsymbol{\sigma}_{\mathbf{k}s}(t) = e^{si(\mathbf{k} \cdot \mathbf{r}_{iA} - \omega_{\mathbf{k}s} t + \arg \xi)} (\delta_{s+} u_{\mathbf{k}} + \delta_{s-} v_{\mathbf{k}}) (\hat{\mathbf{x}} - i\hat{\mathbf{y}}). \quad (\text{S12})$$

Note that only the tranverse components of the spin operator have time-dependent expectation values. This describes the precession of $\langle \mathbf{S}_{iA}(t) \rangle$ around the ordering axis, as one can explicitly see by writing

$$\begin{aligned} \text{Re } \boldsymbol{\sigma}_{\mathbf{k}s} &\propto \text{Re} \left[e^{si(\mathbf{k} \cdot \mathbf{r}_{iA} - \omega_{\mathbf{k}s} t + \arg \xi)} (\hat{\mathbf{x}} - i\hat{\mathbf{y}}) \right] \\ &= \cos(\omega_{\mathbf{k}s} t - \mathbf{k} \cdot \mathbf{r}_{iA} - \arg \xi) \hat{\mathbf{x}} + s \sin(\omega_{\mathbf{k}s} t - \mathbf{k} \cdot \mathbf{r}_{iA} - \arg \xi) \hat{\mathbf{y}}. \end{aligned} \quad (\text{S13})$$

Hence, the sense of the precession depends on s , and we conclude that the two magnon modes have different *chiralities*. A quantity capable of sharply drawing this distinction is the “chirality index”

$$\kappa_s \equiv \text{sgn} \left\{ \left[\langle \mathbf{S}_{iA}(t) \rangle \times \frac{d}{dt} \langle \mathbf{S}_{iA}(t) \rangle \right] \cdot \hat{\mathbf{z}} \right\}, \quad (\text{S14})$$

which is defined based on the time evolution of a spin in a semiclassical picture. Since the cross product in Eq. (S14) is projected onto the ordering direction $\hat{\mathbf{z}}$, we can simply replace \mathbf{S}_{iA} by $\mathbf{S}_{iA}^\perp = S_{iA}^x \hat{\mathbf{x}} + S_{iA}^y \hat{\mathbf{y}}$ when computing κ_s . We find that

$$\begin{aligned} \langle \mathbf{S}_{iA}^\perp(t) \rangle \times \frac{d}{dt} \langle \mathbf{S}_{iA}^\perp(t) \rangle &= \frac{2S}{N_c} |\xi|^2 (\boldsymbol{\sigma}_{\mathbf{k}s} + \boldsymbol{\sigma}_{\mathbf{k}s}^*) \times \frac{d}{dt} (\boldsymbol{\sigma}_{\mathbf{k}s} + \boldsymbol{\sigma}_{\mathbf{k}s}^*) = \frac{4S}{N_c} |\xi|^2 si\omega_{\mathbf{k}s} (\boldsymbol{\sigma}_{\mathbf{k}s} \times \boldsymbol{\sigma}_{\mathbf{k}s}^*) \\ &= \frac{4S}{N_c} |\xi|^2 si\omega_{\mathbf{k}s} (\delta_{s+} u_{\mathbf{k}}^2 + \delta_{s-} v_{\mathbf{k}}^2) (\hat{\mathbf{x}} - i\hat{\mathbf{y}}) \times (\hat{\mathbf{x}} + i\hat{\mathbf{y}}) \\ &= - \left[\frac{8S}{N_c} |\xi|^2 \omega_{\mathbf{k}s} (\delta_{s+} u_{\mathbf{k}}^2 + \delta_{s-} v_{\mathbf{k}}^2) \right] s\hat{\mathbf{z}}. \end{aligned} \quad (\text{S15})$$

Given that $u_{\mathbf{k}}^2 \omega_{\mathbf{k}s}$ and $v_{\mathbf{k}}^2 \omega_{\mathbf{k}s}$ are strictly positive [see Eq. (S5)], we arrive at

$$\boxed{\kappa_s = -s} \quad (\text{if } \xi \neq 0). \quad (\text{S16})$$

The condition $\xi \neq 0$ is guaranteed to hold, e.g., for a coherent state $|\phi_{\mathbf{k}s}\rangle = e^{-|\phi|^2/2} e^{\phi \alpha_{\mathbf{k}s}^\dagger} |0\rangle$, for which $c_n = e^{-|\phi|^2/2} \phi^n / \sqrt{n!}$. On the other hand, states with $\xi = 0$ have a chirality index $\kappa_s = 0$. This occurs, in particular, when $c_n = \delta_{nm} c_m$. In such a case, the precise knowledge of the number of excitations leads to a maximum uncertainty in phase-related variables, which in turn causes the cancellation in the average of the transverse components in Eq. (S11). Finally, note that κ_s otherwise does not depend on the set of coefficients $\{c_n\}$, nor on the momentum \mathbf{k} of the excitation used to construct $|\phi_{\mathbf{k}s}\rangle$.

C. Symmetries of the spin-wave spectrum

In this section, we show why eliminating inversion and translation symmetries that connect different sublattices allows for the splitting of magnon modes with opposite chiralities. The analysis is based on the inspection of symmetries of \mathcal{H}_{LSW} , which not only commute with the Hamiltonian in Eq. (S1), but also leave the reference state for the spin-wave expansion (a Néel state order along the z axis) invariant.

Let $[A|B]$ denote a transformation that acts on spin space with A and in real space with B . Since we ignore relativistic effects, A and B are completely independent, except for when time reversal is applied. In that case, the presence of the time-reversal operator Θ in B must be accompanied by spin inversion \bar{E} in A . Due to the collinearity of the Néel state, one of the symmetries of \mathcal{H}_{LSW} is $T_0 = [\bar{E}C_2|\Theta]$, where $C_2 = e^{-i\pi S_x}$ implements a 180° rotation around the x -axis in spin space. In the absence of J_2 couplings, C_2 can be combined with an inversion \mathcal{P} about the center of a nearest-neighbor bond or a translation \mathbf{t} connecting different sublattices to produce two other symmetries, $T_1 = [C_2|\{\mathcal{P}|\mathbf{0}\}]$ and $T_2 = [C_2|\{E|\mathbf{t}\}]$. The action of these transformations on spin operators is given

$$\begin{aligned} T_0 S_A^z(\mathbf{r}_{iA}) T_0^{-1} &= S_A^z(\mathbf{r}_{iA}), & T_1 S_A^z(\mathbf{r}_{iA}) T_1^{-1} &= S_B^z(\mathcal{P}\mathbf{r}_{iA}), & T_2 S_A^z(\mathbf{r}_{iA}) T_2^{-1} &= S_B^z(\mathbf{r}_{iA} + \mathbf{t}), \\ T_0 S_A^\pm(\mathbf{r}_{iA}) T_0^{-1} &= -S_A^\pm(\mathbf{r}_{iA}), & T_1 S_A^\pm(\mathbf{r}_{iA}) T_1^{-1} &= S_B^\mp(\mathcal{P}\mathbf{r}_{iA}), & T_2 S_A^\pm(\mathbf{r}_{iA}) T_2^{-1} &= S_B^\mp(\mathbf{r}_{iA} + \mathbf{t}). \end{aligned} \quad (\text{S17})$$

By using the Holstein-Primakoff representation, we thus find that

$$T_0 a_{\mathbf{k}} T_0^{-1} = -a_{-\mathbf{k}}, \quad T_1 a_{\mathbf{k}} T_1^{-1} = b_{-\mathbf{k}}, \quad T_2 a_{\mathbf{k}} T_2^{-1} = e^{i\mathbf{k} \cdot \mathbf{t}} b_{\mathbf{k}}. \quad (\text{S18})$$

By using these results, it is easy to derive the transformation properties of the Bogoliubov quasiparticles in Eq. (S4). One finds, for instance, that $T_0 \alpha_{\mathbf{k},s} T_0^{-1} = -\alpha_{-\mathbf{k},s}$ and

$$T_0 \left(\sum_{\mathbf{k}s} \omega_{\mathbf{k}s} \alpha_{\mathbf{k}s}^\dagger \alpha_{\mathbf{k}s} \right) T_0^{-1} = \sum_{\mathbf{k}s} \omega_{\mathbf{k}s} \alpha_{-\mathbf{k}s}^\dagger \alpha_{-\mathbf{k}s} = \sum_{\mathbf{k}s} \omega_{-\mathbf{k}s} \alpha_{\mathbf{k}s}^\dagger \alpha_{\mathbf{k}s}. \quad (\text{S19})$$

Since $T_0 \mathcal{H} T_0^{-1} = \mathcal{H}$, the symmetry T_0 guarantees that $\omega_{\mathbf{k}s} = \omega_{-\mathbf{k},s}$, i.e., the dispersion is inversion-symmetric. Similarly, if T_1 and T_2 were symmetries of the Hamiltonian, then the spectrum would additionally obey the conditions $\omega_{\mathbf{k}s} = \omega_{-\mathbf{k},-s}$ and $\omega_{\mathbf{k}s} = \omega_{\mathbf{k},-s}$. This shows that the degeneracy of magnon bands with opposite chiralities is enforced by T_2 alone or by the combination of T_1 and T_0 . In the altermagnet, none of these options is realized, leading to the splitting of chiral magnons as discussed in the main text.

S2. SU(3) LOCAL-MOMENT ALTERMAGNET ON THE HEXATRIANGULAR LATTICE

In this section, we generalize the approach of the previous section to the SU(3) Heisenberg model discussed in the main text. We present details of the flavor-wave theory and derive the flavor-wave chirality.

In a system where fermions of three different flavors hop on a lattice and form one-third-filled bands, the presence of a strong local Hubbard repulsion gives rise to a Mott insulator where each site is left with a local-moment degree of freedom that transforms under the fundamental representation of the SU(3) algebra [1]. The effective low-energy Hamiltonian then takes the form of an SU(3) Heisenberg model, as in Eq. (1) of the main paper, with bilinear terms $S_{i\mu}^{\beta\alpha} S_{j\nu}^{\beta\alpha} = |\beta_{i\mu}\alpha_{j\nu}\rangle \langle \alpha_{i\mu}\beta_{j\nu}|$ that permute the states at sites $(i\mu)$ and $(j\nu)$ [1, 2]. Specializing this to the hexatriangular lattice, we have

$$\mathcal{H} = \frac{J_1}{3} \sum_{\langle i\mu, j\nu \rangle} S_{i\mu}^{\beta\alpha} S_{j\nu}^{\alpha\beta} + \frac{J_2}{3} \sum_{\langle\langle i\mu, j\mu \rangle\rangle} S_{i\mu}^{\beta\alpha} S_{j\mu}^{\alpha\beta}, \quad (\text{S20})$$

where $J_1, J_2 > 0$ correspond to the solid and dashed couplings depicted in Fig. 1(b) of the main paper.

We note that the $S^{\alpha\beta}$ operators are not the $N^2 - 1 = 8$ independent generators given, in this representation, by one-half of the Gell-Mann matrices $S^n = \lambda_n/2$ [5]. Instead, the relation between these two sets of generators is determined by

$$\begin{aligned} S^{AA} &= \frac{M}{3} \mathbb{1} + S^3 + \frac{1}{\sqrt{3}} S^8, & S^{AB} &= S^1 + iS^2, & S^{BA} &= S^1 - iS^2, \\ S^{BB} &= \frac{M}{3} \mathbb{1} - S^3 + \frac{1}{\sqrt{3}} S^8, & S^{AC} &= S^4 + iS^5, & S^{CA} &= S^4 - iS^5, \\ S^{CC} &= \frac{M}{3} \mathbb{1} - \frac{2}{\sqrt{3}} S^8, & S^{BC} &= S^6 + iS^7, & S^{CB} &= S^6 - iS^7. \end{aligned} \quad (\text{S21})$$

with $M = 1$ and $\mathbb{1}$ the identity matrix. The relations above yield the commutation relation $[S^{\beta\alpha}, S^{\beta'\alpha'}] = S^{\beta\alpha'} \delta_{\alpha\beta'} - S^{\beta'\alpha} \delta_{\alpha'\beta}$ and the condition $\sum_{\alpha} S^{\alpha\alpha} = M$ quoted in the main text.

A. Flavor-wave theory

The ground state of Eq. (S20) is a three-sublattice three-color state [2–4], which can be thought of as the SU(3)-equivalent of a Néel state. The excitations that arise on top of it can be studied within the semiclassical framework of linear flavor-wave theory. To do so, we extend the model above such that the local moments at each site transform under the $(M, 0)$ irreducible representation of the SU(3) algebra, which has dimension $(M+1)(M+2)/2$ and is furnished by completely symmetric tensors with M indices [5]. For a given M , the states of the local Hilbert space correspond to the (nondegenerate) eigenvectors of the two independent diagonal generators of SU(3), S^3 and S^8 , and are conveniently represented in a diagram whose axes are given by the eigenvalues of these operators. The corresponding “weight diagram” for $M = 4$ is shown in Fig. S1.

Similarly to spin-wave theory, flavor-wave theory describes fluctuations about a reference product state $|\psi\rangle$ via an expansion in powers of $1/M$. Here, we expand about $|\psi\rangle = \otimes_{i\mu} |\mu\rangle_{i\mu}$, which is also the product state that minimizes $\langle \mathcal{H} \rangle$ [2]. For indices $\alpha, \beta \neq \mu$, the appropriate Holstein-Primakoff representation reads:

$$\begin{aligned} S_{i\mu}^{\mu\mu} &= M - \sum_{\beta \neq \mu} a_{i\mu\beta}^\dagger a_{i\mu\beta}, & S_{i\mu}^{\mu\alpha} &= \sqrt{M - \sum_{\beta \neq \mu} a_{i\mu\beta}^\dagger a_{i\mu\beta}} a_{i\mu\alpha} \approx \sqrt{M} a_{i\mu\alpha}, \\ S_{i\mu}^{\alpha\beta} &= a_{i\mu\alpha}^\dagger a_{i\mu\beta}, & S_{i\mu}^{\alpha\mu} &= a_{i\mu\alpha}^\dagger \sqrt{M - \sum_{\beta \neq \mu} a_{i\mu\beta}^\dagger a_{i\mu\beta}} \approx \sqrt{M} a_{i\mu\alpha}^\dagger. \end{aligned} \quad (\text{S22})$$

In terms of Fig. S1, $a_{i\mu\beta}^\dagger$ creates a boson that moves the state of the “spin” at site $(i\mu)$ one step closer from $|\beta\rangle$ along a line parallel to the edge of $\overline{\mu\beta}$ of the diagram. Given that there are two such bosonic species per sublattice, the system will have six magnon bands in total.

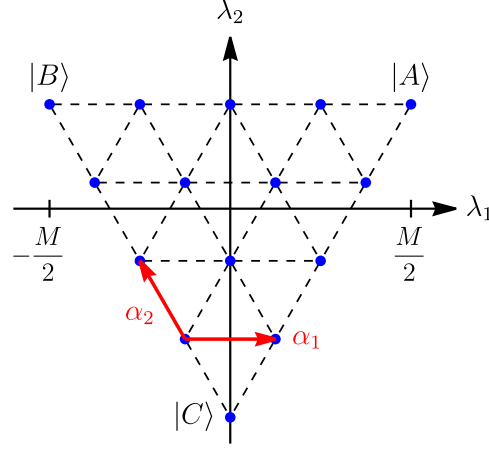


FIG. S1. Weight diagram of the $(4, 0)$ totally symmetric irreducible representation of the $SU(3)$ algebra. λ_1 and λ_2 correspond to the eigenvalues of the independent diagonal generators of $SU(3)$, which can be expressed as $S^3 = (S^{AA} - S^{BB})/2$ and $S^8 = \sqrt{3}(S^{AA} + S^{BB})/2 - M/\sqrt{3}$, respectively. The maximum weight state $|A\rangle$ corresponds to a fully polarized moment along the A direction, and its Weyl reflections yield the two complementary states $|B\rangle$ and $|C\rangle$.

The operator product appearing in the J_2 term of Eq. (S22) thus becomes

$$\begin{aligned} \sum_{\alpha\beta} S_{i\mu}^{\beta\alpha} S_{j\mu}^{\alpha\beta} &= S_{i\mu}^{\mu\mu} S_{j\mu}^{\mu\mu} + \sum_{\alpha \neq \mu} (S_{i\mu}^{\mu\alpha} S_{j\mu}^{\alpha\mu} + S_{i\mu}^{\alpha\mu} S_{j\mu}^{\mu\alpha}) + \mathcal{O}(M^0) \\ &= M^2 - M \sum_{\alpha \neq \mu} (a_{i\mu\alpha}^\dagger a_{i\mu\alpha} + a_{j\mu\alpha}^\dagger a_{j\mu\alpha}) + M \sum_{\alpha \neq \mu} (a_{i\mu\alpha} a_{j\mu\alpha}^\dagger + a_{i\mu\alpha}^\dagger a_{j\mu\alpha}) + \mathcal{O}(M^0). \end{aligned} \quad (\text{S23})$$

Now let $\nu \neq \mu$. The product in the J_1 term reads

$$\begin{aligned} \sum_{\alpha\beta} S_{i\mu}^{\beta\alpha} S_{j\nu}^{\alpha\beta} &= S_{i\mu}^{\mu\mu} S_{j\nu}^{\mu\mu} + S_{i\mu}^{\nu\nu} S_{j\nu}^{\nu\nu} + S_{i\mu}^{\mu\nu} S_{j\nu}^{\nu\mu} + S_{i\mu}^{\nu\mu} S_{j\nu}^{\mu\nu} + \mathcal{O}(M^0) \\ &= M (a_{j\nu\mu}^\dagger a_{j\nu\mu} + a_{i\mu\nu}^\dagger a_{i\mu\nu} + a_{i\mu\nu} a_{j\nu\mu} + a_{i\mu\nu}^\dagger a_{j\nu\mu}^\dagger) + \mathcal{O}(M^0). \end{aligned} \quad (\text{S24})$$

Substituting back into the Eq. (S20), we obtain

$$\begin{aligned} \mathcal{H}_{\text{LFW}} &= N_s M^2 \frac{J_2}{3} + J_1 M \sum_{\mathbf{k}\mu} \left[a_{\mathbf{k},\mu,\mu+1}^\dagger a_{\mathbf{k},\mu,\mu+1} + a_{\mathbf{k},\mu+1,\mu}^\dagger a_{\mathbf{k},\mu+1,\mu} + \left(\tilde{\gamma}_{\mathbf{k}} a_{\mathbf{k},\mu,\mu+1}^\dagger a_{-\mathbf{k},\mu+1,\mu}^\dagger + \text{h.c.} \right) \right] \\ &\quad - \frac{2}{3} J_2 M \sum_{\mathbf{k}\mu} \sum_{\alpha \neq \mu} \tilde{\Gamma}_{\mathbf{k}\mu} a_{\mathbf{k},\mu,\alpha}^\dagger a_{\mathbf{k},\mu,\alpha}, \end{aligned} \quad (\text{S25})$$

Here, as in the main text, we adopted the notation $\{A, B, C\} \equiv \{1, 2, 3\} \bmod 3$ and introduced the functions $\tilde{\gamma}_{\mathbf{k}} = \frac{1}{3} \sum_{\delta_1} e^{i\mathbf{k} \cdot \delta_1}$ and $\tilde{\Gamma}_{\mathbf{k}\mu} = 1 - \cos(\mathbf{k} \cdot \delta_{2\mu})$. Explicitly, the nearest-neighbor vectors read

$$\delta_1 \in \left\{ \left(-1/2, \sqrt{3}/2 \right), \left(-1/2, -\sqrt{3}/2 \right), (1, 0) \right\} \quad (\text{S26})$$

and the sublattice-specific second-neighbor vectors are

$$\delta_{2A} = (0, \sqrt{3}), \quad \delta_{2B} = (3, \sqrt{3})/2, \quad \delta_{2C} = (3, -\sqrt{3})/2. \quad (\text{S27})$$

By using bosonic commutation relations and exploiting the fact that the Brillouin zone is symmetric under inversion, we can express the Hamiltonian as a sum of three 2×2 blocks

$$\mathcal{H}_{\text{LFW}} = N_s \left[\frac{M^2 J_2}{3} - M J_1 (1 - 2\tilde{\eta}) \right] + M J_1 \sum_{\mathbf{k}\mu} \begin{pmatrix} a_{\mathbf{k},\mu,\mu+1}^\dagger & a_{-\mathbf{k},\mu+1,\mu} \end{pmatrix} \begin{pmatrix} 1 - 2\tilde{\eta}\tilde{\Gamma}_{\mathbf{k}\mu} & \tilde{\gamma}_{\mathbf{k}} \\ \tilde{\gamma}_{\mathbf{k}}^* & 1 - 2\tilde{\eta}\tilde{\Gamma}_{\mathbf{k},\mu+1} \end{pmatrix} \begin{pmatrix} a_{\mathbf{k},\mu,\mu+1} \\ a_{-\mathbf{k},\mu+1,\mu}^\dagger \end{pmatrix}, \quad (\text{S28})$$

with $\tilde{\eta} = J_2/(3J_1)$. This block structure implies that each collective mode acts *exclusively* on two sublattices. Building on this insight, we redefine the label μ such that it labels the sublattice which does *not* appear in a given term of the Hamiltonian. With this relabelling, the bilinear piece of Eq. (S28) is identical to Eq. (4) of the main text.

After a Bogoliubov transformation, Eq. (S28) becomes

$$\mathcal{H}_{\text{LFW}} = \frac{N_s}{3} [M^2 J_2 - 3M J_1 (1 - 2\tilde{\eta})] + \sum_{\mathbf{k}\mu} \sum_{s=\pm} \omega_{\mathbf{k}\mu s} \left(\alpha_{\mathbf{k}\mu s}^\dagger \alpha_{\mathbf{k}\mu s} + \frac{1}{2} \right), \quad (\text{S29})$$

where $\omega_{\mathbf{k}\mu\pm}$ are given by Eq. (5) of the main text. The magnon operators are related to the Holstein-Primakoff bosons via

$$\begin{pmatrix} a_{\mathbf{k},\mu+1,\mu-1} \\ a_{-\mathbf{k},\mu-1,\mu+1}^\dagger \end{pmatrix} = \begin{pmatrix} u_{\mathbf{k}\mu} & v_{\mathbf{k}\mu} e^{i\varphi_{\mathbf{k}}} \\ v_{\mathbf{k}\mu} e^{-i\varphi_{\mathbf{k}}} & u_{\mathbf{k}\mu} \end{pmatrix} \begin{pmatrix} \alpha_{\mathbf{k},\mu,+} \\ \alpha_{-\mathbf{k},\mu,-}^\dagger \end{pmatrix} \quad (\text{S30})$$

with $\varphi_{\mathbf{k}} = \arg \tilde{\gamma}_{\mathbf{k}}$. If we define the function

$$D_{\mathbf{k}\mu} = \frac{|\tilde{\gamma}_{\mathbf{k}}|}{1 - \frac{J_2}{3J_1} (\tilde{\Gamma}_{\mathbf{k},\mu-1} + \tilde{\Gamma}_{\mathbf{k},\mu+1})}, \quad (\text{S31})$$

then the Bogoliubov coefficients in Eq. (S30) can be written as

$$u_{\mathbf{k}\mu} = \frac{1}{\sqrt{2}} \left(\frac{1}{\sqrt{1 - D_{\mathbf{k}\mu}^2}} + 1 \right)^{1/2}, \quad v_{\mathbf{k}\mu} = -\frac{1}{\sqrt{2}} \left(\frac{1}{\sqrt{1 - D_{\mathbf{k}\mu}^2}} - 1 \right)^{1/2}. \quad (\text{S32})$$

B. Flavor-wave chirality

We are now in the position to study the dynamics of the SU(3) spin degrees of freedom in an excited state

$$|\phi_{\mathbf{k}\mu s}\rangle = \sum_{n=0}^{\infty} c_n |n_{\mathbf{k}\mu s}\rangle = \sum_{n=0}^{\infty} \frac{c_n}{\sqrt{n!}} \left(\alpha_{\mathbf{k}\mu s}^\dagger \right)^n |0\rangle, \quad (\text{S33})$$

where $|0\rangle$ stands for the ground state of Eq. (S29). To begin, consider the expectation value of the nine operators belonging to a site $i\mu$:

$$\begin{aligned} \langle S_{i\mu}^{\lambda\lambda'}(t) \rangle &\equiv \langle \phi_{\mathbf{k}\mu s} | S_{i\mu}^{\lambda\lambda'}(t) | \phi_{\mathbf{k}\mu s} \rangle = \sum_{m,n} c_m^* c_n \langle m_{\mathbf{k}\mu s} | S_{i\mu}^{\lambda\lambda'}(t) | n_{\mathbf{k}\mu s} \rangle \\ &= \sum_{m,n} \frac{c_m^* c_n}{\sqrt{m!n!}} \langle 0 | S_{i\mu}^{\lambda\lambda'}(t) (\alpha_{\mathbf{k}\mu s})^m (\alpha_{\mathbf{k}\mu s}^\dagger)^n | 0 \rangle = \langle 0 | S_{i\mu}^{\lambda\lambda'}(t) | 0 \rangle \sum_{n=0}^{\infty} |c_n|^2 \\ &= \delta_{\lambda\lambda'} \left[\delta_{\lambda\mu} \left\langle 0 \left| M - \sum_{\alpha \neq \mu} a_{i\mu\alpha}^\dagger(t) a_{i\mu\alpha}(t) \right| 0 \right\rangle + (1 - \delta_{\lambda\mu}) \left\langle 0 \left| a_{i\mu\lambda}^\dagger(t) a_{i\mu\lambda}(t) \right| 0 \right\rangle \right] \\ &= \delta_{\lambda\lambda'} [\delta_{\lambda\mu} (M - 2m_\perp) + (1 - \delta_{\lambda\mu}) m_\perp]. \end{aligned} \quad (\text{S34})$$

In going from the first to second line, we used the fact that the Holstein-Primakoff bosons related to $S_{i\mu}^{\lambda\lambda'}$ necessarily have a subindex μ . Thus, by virtue Eq. (S30), $[S_{i\mu}^{\lambda\lambda'}, \alpha_{\mathbf{k}\mu s}] = [S_{i\mu}^{\lambda\lambda'}, \alpha_{\mathbf{k}\mu s}^\dagger] = 0$ for every λ, λ' and we are left only with expectation values with respect to the ground state $|0\rangle$. This tells us that the result is time-independent, which was to be expected in the first place, since the excitations created by $\alpha_{\mathbf{k}\mu s}^\dagger$ do not affect the spins on sublattice μ . In the last step, we identified $m_\perp = \langle 0 | S_{i\mu}^{\alpha\alpha} | 0 \rangle = \langle 0 | a_{i\mu\alpha}^\dagger a_{i\mu\alpha} | 0 \rangle$ as the fluctuation-induced magnetization along the complementary flavors $\alpha \neq \mu$. By symmetry, m_\perp will be the same for both α . Written explicitly,

$$m_\perp = \frac{1}{N_c} \sum_{\mathbf{p}\mathbf{q}} v_{\mathbf{q},\mu-1} v_{\mathbf{p},\mu-1} e^{i(\varphi_{\mathbf{p}} - \varphi_{\mathbf{q}})} \langle 0 | \alpha_{-\mathbf{q},\mu-1,-} \alpha_{-\mathbf{p},\mu-1,-}^\dagger | 0 \rangle = \frac{1}{N_c} \sum_{\mathbf{p}} v_{\mathbf{p},\mu-1}^2. \quad (\text{S35})$$

Our previous calculation confirmed that excitations created by $\alpha_{\mathbf{k}\mu s}^\dagger$ only generate dynamical behavior on sublattices $\mu \pm 1$. Thus, let us now consider expectation values of the type $\langle S_{i,\mu+1}^{\lambda\lambda'}(t) \rangle$. As we will show below, the nontrivial time dependence arises from combinations of λ and λ' included in

$$s^x = \frac{S^{\mu+1,\mu-1} + S^{\mu-1,\mu+1}}{2}, \quad s^y = \frac{S^{\mu+1,\mu-1} - S^{\mu-1,\mu+1}}{2i}, \quad s^z = \frac{S^{\mu+1,\mu+1} - S^{\mu-1,\mu-1}}{2}, \quad (\text{S36})$$

all defined on site $(i, \mu + 1)$. We note that the large- M three-color reference state $|\psi\rangle$ has $\langle s^z \rangle = M/2$ and $\langle s^x \rangle = \langle s^y \rangle = 0$. By using the commutation relations of the $S^{\alpha\beta}$, one can show that the operators above form an $\text{SU}(2)$ subalgebra for $\text{SU}(3)$. For instance,

$$[s^x, s^y] = \frac{i}{2} [S^{\mu+1,\mu-1}, S^{\mu-1,\mu+1}] = \frac{i}{2} (S^{\mu+1,\mu+1} - S^{\mu-1,\mu-1}) = i s^z. \quad (\text{S37})$$

$$\begin{aligned} [s^x, s^z] &= \frac{1}{4} ([S^{\mu+1,\mu-1}, S^{\mu+1,\mu+1}] - [S^{\mu+1,\mu-1}, S^{\mu-1,\mu-1}] + [S^{\mu-1,\mu+1}, S^{\mu+1,\mu+1}] - [S^{\mu-1,\mu+1}, S^{\mu-1,\mu-1}]) \\ &= \frac{1}{2} (-S^{\mu+1,\mu-1} + S^{\mu-1,\mu+1}) = -i s^y. \end{aligned} \quad (\text{S38})$$

Now consider

$$\begin{aligned} \langle s_{i,\mu+1}^+(t) \rangle &\equiv \langle \phi_{\mathbf{k}\mu s} | S_{i,\mu+1}^{\mu+1,\mu-1}(t) | \phi_{\mathbf{k}\mu s} \rangle \approx \sqrt{M} \sum_{m,n} c_m^* c_n \langle m_{\mathbf{k}\mu s} | a_{i,\mu+1,\mu-1}(t) | n_{\mathbf{k}\mu s} \rangle \\ &= \sqrt{\frac{M}{N_c}} \sum_{m,n} c_m^* c_n \sum_{\mathbf{q}} e^{i\mathbf{q} \cdot \mathbf{r}_{i,\mu+1}} \langle m_{\mathbf{k}\mu s} | u_{\mathbf{q}\mu} \alpha_{\mathbf{q}\mu+}(t) + v_{\mathbf{q}\mu} e^{i\varphi_{\mathbf{q}}} \alpha_{-\mathbf{q}\mu-}^\dagger(t) | n_{\mathbf{k}\mu s} \rangle \\ &= \sqrt{\frac{M}{N_c}} e^{si(\mathbf{k} \cdot \mathbf{r}_{i,\mu+1} - \omega_{\mathbf{k}\mu s} t)} \sum_{m,n} c_m^* c_n (\delta_{s+} \delta_{n,m+1} \sqrt{n} u_{\mathbf{k}\mu} + \delta_{s-} \delta_{m,n+1} \sqrt{n+1} v_{\mathbf{k}\mu} e^{i\varphi_{\mathbf{k}}}) \\ &= \sqrt{\frac{M}{N_c}} e^{si(\mathbf{k} \cdot \mathbf{r}_{i,\mu+1} - \omega_{\mathbf{k}\mu s} t)} \left[\delta_{s+} u_{\mathbf{k}\mu} \left(\sum_{m=0}^{\infty} \sqrt{m+1} c_m^* c_{m+1} \right) + \delta_{s-} v_{\mathbf{k}\mu} e^{i\varphi_{\mathbf{k}}} \left(\sum_{n=0}^{\infty} \sqrt{n+1} c_{n+1}^* c_n \right) \right] \\ &= \sqrt{\frac{M}{N_c}} |\xi| e^{si(\mathbf{k} \cdot \mathbf{r}_{i,\mu+1} - \omega_{\mathbf{k}\mu s} t + \arg \xi)} (\delta_{s+} u_{\mathbf{k}\mu} + \delta_{s-} v_{\mathbf{k}\mu} e^{i\varphi_{\mathbf{k}}}), \end{aligned} \quad (\text{S39})$$

where $N_c = N_s/3$ denotes the number of unit cells and ξ is defined as in the $\text{SU}(2)$ case [see Eq. (S8)]. Similarly,

$$\begin{aligned} \langle s_{i,\mu+1}^z(t) \rangle &\equiv \frac{1}{2} \langle \phi_{\mathbf{k}\mu s} | S_{i,\mu+1}^{\mu+1,\mu+1}(t) - S_{i,\mu+1}^{\mu-1,\mu-1}(t) | \phi_{\mathbf{k}\mu s} \rangle \\ &\approx \frac{M}{2} - \langle a_{i,\mu+1,\mu}^\dagger(t) a_{i,\mu+1,\mu}(t) \rangle - 2 \langle a_{i,\mu+1,\mu-1}^\dagger(t) a_{i,\mu+1,\mu-1}(t) \rangle \\ &= \frac{M}{2} - \langle 0 | a_{i,\mu+1,\mu}^\dagger a_{i,\mu+1,\mu} | 0 \rangle - \frac{2}{N_c} \sum_{\mathbf{p}\mathbf{q}} e^{i(\mathbf{p}-\mathbf{q}) \cdot \mathbf{r}_{i,\mu+1}} \langle a_{\mathbf{q},\mu+1,\mu-1}^\dagger(t) a_{\mathbf{p},\mu+1,\mu-1}(t) \rangle \\ &= \frac{M}{2} - m_\perp - \frac{2}{N_c} \sum_{\mathbf{p}\mathbf{q}} e^{i(\mathbf{p}-\mathbf{q}) \cdot \mathbf{r}_{i,\mu+1}} \sum_{m,n} c_m^* c_n \langle m_{\mathbf{k}\mu s} | a_{\mathbf{q},\mu+1,\mu-1}^\dagger(t) a_{\mathbf{p},\mu+1,\mu-1}(t) | n_{\mathbf{k}\mu s} \rangle. \end{aligned} \quad (\text{S40})$$

The last expectation value yields the same kind of expression that appears in Eq. (S9), such that

$$\begin{aligned} \langle s_{i,\mu+1}^z(t) \rangle &= \frac{M}{2} - m_\perp - \frac{2}{N_c} \sum_n |c_n|^2 \sum_{\mathbf{p}} [\delta_{s+} \delta_{\mathbf{p}\mathbf{k}} u_{\mathbf{k}\mu}^2 n + v_{\mathbf{p}\mu}^2 (1 + \delta_{s-} \delta_{\mathbf{p},-\mathbf{k}} n)] \\ &= \frac{M}{2} - 3m_\perp - \frac{2\zeta}{N_c} (\delta_{s+} u_{\mathbf{k}\mu}^2 + \delta_{s-} v_{\mathbf{k}\mu}^2), \end{aligned} \quad (\text{S41})$$

where $\zeta = \zeta(\{c_n\})$ is also defined as before.

Now let us consider expectation values of the six remaining operators, which do not belong to the $\text{SU}(2)$ subalgebra defined above. The easiest cases are

$$\langle S_{i,\mu+1}^{\mu-1,\mu}(t) \rangle = \langle a_{i,\mu+1,\mu-1}^\dagger(t) a_{i,\mu+1,\mu}(t) \rangle = 0, \quad \langle S_{i,\mu+1}^{\mu+1,\mu}(t) \rangle \approx \sqrt{M} \langle a_{i,\mu+1,\mu}(t) \rangle = 0. \quad (\text{S42})$$

which vanish because $a_{i,\mu+1,\mu}$ can be written as a linear combination of $\alpha_{\mathbf{q},\mu-1,s}$ ($\alpha_{\mathbf{q},\mu-1,s}^\dagger$) operators. When commuted up to $|0\rangle$ ($\langle 0|$), the latter just yield zero. This leaves us with two cases: $(\lambda, \lambda') = (\mu, \mu)$ and $(\mu-1, \mu-1)$. The results are

$$\begin{aligned} \langle S_{i,\mu+1}^{\mu,\mu}(t) \rangle &= \langle a_{i,\mu+1,\mu}^\dagger(t) a_{i,\mu+1,\mu}(t) \rangle \\ &= \frac{1}{N_c} \sum_{\mathbf{p}\mathbf{q}} e^{i(\mathbf{p}-\mathbf{q})\cdot\mathbf{r}_{i,\mu+1}} \langle [v_{\mathbf{q},\mu-1} e^{-i\varphi_{\mathbf{q}}} \alpha_{-\mathbf{q},\mu-1,-}(t)] [v_{\mathbf{p},\mu-1} e^{i\varphi_{\mathbf{p}}} \alpha_{-\mathbf{p},\mu-1,-}^\dagger(t)] \rangle = m_\perp \end{aligned} \quad (\text{S43})$$

and

$$\begin{aligned} \langle S_{i,\mu+1}^{\mu-1,\mu-1}(t) \rangle &= \langle a_{i,\mu+1,\mu-1}^\dagger(t) a_{i,\mu+1,\mu-1}(t) \rangle \\ &= \frac{1}{N_c} \sum_{\mathbf{p}\mathbf{q}} e^{i(\mathbf{p}-\mathbf{q})\cdot\mathbf{r}_{i,\mu+1}} \langle u_{\mathbf{q}\mu} u_{\mathbf{p}\mu} \alpha_{\mathbf{q}\mu+}^\dagger(t) \alpha_{\mathbf{p}\mu+}(t) + v_{\mathbf{q}\mu} v_{\mathbf{p}\mu} e^{i(\varphi_{\mathbf{p}} - \varphi_{\mathbf{q}})} \alpha_{-\mathbf{q},\mu,-}(t) \alpha_{-\mathbf{p},\mu,-}^\dagger(t) \rangle \\ &= m_\perp + \sum_{\mathbf{p}\mathbf{q}} \frac{e^{i(\mathbf{p}-\mathbf{q})\cdot\mathbf{r}_{i,\mu+1}}}{N_c} \langle u_{\mathbf{q}\mu} u_{\mathbf{p}\mu} \alpha_{\mathbf{q}\mu+}^\dagger(t) \alpha_{\mathbf{p}\mu+}(t) + v_{\mathbf{q}\mu} v_{\mathbf{p}\mu} e^{i(\varphi_{\mathbf{p}} - \varphi_{\mathbf{q}})} \alpha_{-\mathbf{p},\mu,-}^\dagger(t) \alpha_{-\mathbf{q},\mu,-}(t) \rangle \\ &= m_\perp + \frac{\zeta}{N_c} (\delta_{s+} u_{\mathbf{k}\mu}^2 + \delta_{s-} v_{\mathbf{k}\mu}^2). \end{aligned} \quad (\text{S44})$$

Hence, we have proven our earlier claim that the dynamical behavior generated by $\alpha_{\mathbf{k}\mu s}^\dagger$ magnons manifests only in an $\text{SU}(2)$ subalgebra of $\text{SU}(3)$. This allows us to define the chirality of the flavor-wave modes as

$$\kappa_{\mu s} \equiv \text{sgn} \left\{ \left[\langle \mathbf{s}_{i,\mu+1}(t) \rangle \times \frac{d}{dt} \langle \mathbf{s}_{i,\mu+1}(t) \rangle \right] \cdot \hat{\mathbf{z}} \right\}. \quad (\text{S45})$$

where $\mathbf{s} = (s^x, s^y, s^z)$, and $\hat{\mathbf{z}}$ corresponds to the axis of precession. The choice of the reference site $(i, \mu+1)$ is of course arbitrary, and an equally valid definition would be to replace $(\mu+1) \rightarrow (\mu-1)$. However, the sole effect of this modification is to invert the chirality of every single mode μs . This clarifies that the chirality index of a single mode does not carry physical significance on its own; only differences in chiralities are meaningful. A calculation analogous to the one sketched after Eq. (S14) yields

$$\boxed{\kappa_{\mu s} = -s} \quad (\text{if } \xi \neq 0). \quad (\text{S46})$$

In other words, the modes with dispersion $\omega_{\mathbf{k}\mu s}$, which are split by a $J_2 \neq 0$, have different chiralities.

C. Spin point group and symmetries of the flavor-wave spectrum

We conclude this section with an analysis of the symmetries of the flavor-wave dispersion in order to rationalize the partial degeneracies and crossings seen in Fig. 2(b) of the main paper.

Similarly to the $\text{SU}(2)$ case, the fact that the dispersion is inversion-symmetric, i.e., $\omega_{\mathbf{k}\mu s} = \omega_{-\mathbf{k}\mu s}$, follows from a symmetry $T_0 = [B_0 | \Theta]$, where B_0 is a transformation that (including the effects of time reversal) leaves the three-color state invariant.

Additional symmetries of the spectrum are associated with the nontrivial spin point group of the system, i.e., the set of elements that combine point group operations with independent transformations in spin space to leave both the Hamiltonian and the magnetic state invariant. The term “nontrivial” here refers to the fact that, apart from the identity $[E | E]$, we only consider transformations that necessarily affect real space. Generally, the number and types of allowed spin point groups in a given system are restricted by lattice symmetries and can be fully categorized as follows [7, 8]. One starts by identifying the point group \mathbf{G} of the underlying lattice and constructing all normal subgroups $\mathbf{H}_a \subset \mathbf{G}$, i.e., the subgroups that fulfill $g\mathbf{H}_a g^{-1} = \mathbf{H}_a$, $\forall g \in \mathbf{G}$. This leads to a series of quotient groups $\mathbf{G}/\mathbf{H}_a = \{\mathbf{H}_a, g_2\mathbf{H}_a, \dots, g_n\mathbf{H}_a\}$ of order $n = N(\mathbf{G})/N(\mathbf{H}_a)$. For each a , one can find a subgroup $\mathbf{B}_a = \{E, B_2, \dots, B_n\}$ of operations in spin space that is isomorphic to \mathbf{G}/\mathbf{H}_a . A spin point group $\mathbf{R}_s^{(a)}$ is then formed by pairwise composition of the elements of both subgroups:

$$\mathbf{R}_s^{(a)} = [E | \mathbf{H}_a] + [B_2 | g_2\mathbf{H}_a] + \dots + [B_n | g_n\mathbf{H}_a]. \quad (\text{S47})$$

The spatial symmetries of the hexatriangular lattice are fully described by the wallpaper group $p31m$, whose associated point group is $\mathbf{G} = D_3$, i.e., the set of transformations that leave an equilateral triangle invariant. These operations can be applied with respect to the center of any filled triangle of Fig. 1(b) of the main text. If R denotes a counterclockwise rotation by 120° and M_μ is a reflection that exchanges sublattices $\mu - 1$ and $\mu + 1$, then

$$\mathbf{G} = D_3 = \{E, R, R^2, M_A, M_B, M_C\}. \quad (\text{S48})$$

The normal subgroups of \mathbf{G} and the resulting quotient groups are

$$\mathbf{H}_1 = \mathbf{G}, \quad \mathbf{G}/\mathbf{H}_1 = \{\mathbf{H}_1\}, \quad (\text{S49})$$

$$\mathbf{H}_2 = \{E, R, R^2\} \cong C_3, \quad \mathbf{G}/\mathbf{H}_2 = \{\mathbf{H}_2, M_A \mathbf{H}_2\} \cong Z_2, \quad (\text{S50})$$

$$\mathbf{H}_3 = \{E\}, \quad \mathbf{G}/\mathbf{H}_3 = \{\mathbf{H}_3, R \mathbf{H}_3, R^2 \mathbf{H}_3, M_A \mathbf{H}_3, M_B \mathbf{H}_3, M_C \mathbf{H}_3\} \cong S_3, \quad (\text{S51})$$

where we have used the symbol \cong to indicate isomorphisms between groups. In particular, the $SU(3)$ altermagnetic phase corresponds to

$$\mathbf{R}_s^{(3)} = [E||E] + [(ABC)||R] + [(ACB)||R^2] + [(BC)||M_A] + [(AC)||M_B] + [(AB)||M_C]. \quad (\text{S52})$$

The operators on the left-hand side of the double bars stand for $SU(3)$ transformations that permute the colors in the specified way. We have, for instance, that $(BC) = e^{-i\pi S^6}$.

Now consider the transformation $T_A = [(BC)||M_A]$, which acts on the $SU(3)$ generators as $T_A S_\mu^{\alpha\beta}(\mathbf{r}_{i\mu}) T_A^{-1} = S_{\tilde{\mu}}^{\tilde{\alpha}\tilde{\beta}}(M_A \mathbf{r}_{i\mu})$, with $(\tilde{A}, \tilde{B}, \tilde{C}) = (A, C, B)$. Thus, by using Eq. (S22), we obtain

$$T_A a_{\mu\beta}(\mathbf{r}_{i\mu}) T_A^{-1} = a_{\tilde{\mu}\tilde{\beta}}(M_A \mathbf{r}_{i\mu}), \quad (\text{S53})$$

$$T_A a_{\mathbf{k}\mu\beta} T_A^{-1} = \frac{1}{\sqrt{N_c}} \sum_i e^{-i\mathbf{k}\cdot\mathbf{r}_{i\mu}} a_{\tilde{\mu}\tilde{\beta}}(M_A \mathbf{r}_{i\mu}) = \frac{1}{\sqrt{N_c}} \sum_j e^{-i(M_A \mathbf{k})\cdot\mathbf{r}_{j\tilde{\mu}}} a_{\tilde{\mu}\tilde{\beta}}(\mathbf{r}_{j\tilde{\mu}}) = a_{\tilde{\mathbf{k}}\tilde{\mu}\tilde{\beta}}, \quad (\text{S54})$$

where we have introduced the shorthand notation $\tilde{\mathbf{k}} = M_A \mathbf{k}$. We shall now apply this transformation to the Hamiltonian $\mathcal{H} = \sum_{\mathbf{k}\mu} \Psi_{\mathbf{k}\mu}^\dagger \mathbb{M}_{\mathbf{k}\mu} \Psi_{\mathbf{k}\mu}$ and manipulate the result so as to restore its original form. The ensuing changes to the matrices $\mathbb{M}_{\mathbf{k}\mu}$ will then allow us to infer the symmetries of the spectrum. Starting with the 2×2 block $\mu = A$:

$$\begin{aligned} \sum_{\mathbf{k}} \Psi_{\mathbf{k}A}^\dagger \mathbb{M}_{\mathbf{k}A} \Psi_{\mathbf{k}A} &= \sum_{\mathbf{k}} \left[A_{\mathbf{k}A} a_{\mathbf{k}BC}^\dagger a_{\mathbf{k}BC} + B_{\mathbf{k}A} a_{-\mathbf{k}CB} a_{-\mathbf{k}CB}^\dagger + \left(C_{\mathbf{k}} a_{\mathbf{k}BC}^\dagger a_{-\mathbf{k}CB}^\dagger + \text{h.c.} \right) \right] \\ &\mapsto \sum_{\mathbf{k}} \left[A_{\mathbf{k}A} a_{\tilde{\mathbf{k}}CB}^\dagger a_{\tilde{\mathbf{k}}CB} + B_{\mathbf{k}A} a_{-\tilde{\mathbf{k}}BC} a_{-\tilde{\mathbf{k}}BC}^\dagger + \left(C_{\mathbf{k}} a_{\tilde{\mathbf{k}}CB}^\dagger a_{-\tilde{\mathbf{k}}BC}^\dagger + \text{h.c.} \right) \right] \\ &= \sum_{\mathbf{k}} \left[A_{-\tilde{\mathbf{k}}A} a_{-\mathbf{k}CB} a_{-\mathbf{k}CB}^\dagger + B_{-\tilde{\mathbf{k}}A} a_{\mathbf{k}BC}^\dagger a_{\mathbf{k}BC} + \left(C_{-\tilde{\mathbf{k}}} a_{\mathbf{k}BC}^\dagger a_{-\mathbf{k}CB}^\dagger + \text{h.c.} \right) \right] + \sum_{\mathbf{k}} (B_{\mathbf{k}A} - A_{\mathbf{k}A}) \\ &= \sum_{\mathbf{k}} \Psi_{\mathbf{k}A}^\dagger \begin{pmatrix} B_{-\tilde{\mathbf{k}}A} & C_{-\tilde{\mathbf{k}}} \\ C_{-\tilde{\mathbf{k}}}^* & A_{-\tilde{\mathbf{k}}A} \end{pmatrix} \Psi_{\mathbf{k}A}. \end{aligned} \quad (\text{S55})$$

To arrive at the last line, we used the fact that $\sum_{\mathbf{k}} (B_{\mathbf{k}A} - A_{\mathbf{k}A}) = 0$ due to symmetry. Similarly,

$$\sum_{\mathbf{k}} \Psi_{\mathbf{k}B}^\dagger \mathbb{M}_{\mathbf{k}B} \Psi_{\mathbf{k}B} \mapsto \sum_{\mathbf{k}} \Psi_{\mathbf{k}C}^\dagger \begin{pmatrix} B_{-\tilde{\mathbf{k}}B} & C_{-\tilde{\mathbf{k}}} \\ C_{-\tilde{\mathbf{k}}}^* & A_{-\tilde{\mathbf{k}}B} \end{pmatrix} \Psi_{\mathbf{k}C}. \quad (\text{S56})$$

Equations (S55), and (S56) then lead to

$$\omega_{\mathbf{k}\mu s} = \omega_{-\tilde{\mathbf{k}}, \tilde{\mu}, -s}. \quad (\text{S57})$$

Hence, the symmetries T_0 and T_A together imply that the flavor-wave modes labelled by (μ, s) and $(\tilde{\mu}, -s)$ are mapped onto each other under $(k_x, k_y) \mapsto (\pm k_x, \mp k_y)$. This enforces a series of band crossings along the lines $k_x = 0$ and $k_y = 0$, as seen in Fig. 1(c,d) in the main text, as well as along the vertical boundaries of the Brillouin zone. Similar conclusions follow if one considers symmetry operations related to T_A by a 120° rotation in real space and a suitable permutation of the flavor indices. In full generality,

$$\omega_{\mathbf{k}\mu s} = \omega_{-\mathbf{k}, \mu, s} = \omega_{M_\mu \mathbf{k}, P_\mu \mu, -s}, \quad (\text{S58})$$

where P_μ is a simple permutation of (A, B, C) that exchanges $\mu - 1$ and $\mu + 1$. Equation (S58) captures all of the crossings between modes of opposite chirality which are highlighted in Fig. 1(d) of the main text.

S3. ALTERMAGNETIC KONDO-LATTICE MODELS AND FLAVOR-SPLIT BANDS

In this section we present details concerning the electronic altermagnetic models discussed in the main text.

A. SU(2) checkerboard Kondo-lattice model

For SU(2) the Kondo-lattice model of Eq. (8) in the main text takes the form

$$\mathcal{H}_K = - \sum_{i\mu, j\nu} \left(t_{i\mu, j\nu} c_{i\mu\alpha}^\dagger c_{j\nu\alpha} + \text{h.c.} \right) - \frac{K}{4S} \sum_{i\mu} \mathbf{S}_{i\mu} \cdot \left(c_{i\mu\alpha}^\dagger \boldsymbol{\sigma}_{\alpha\beta} c_{i\mu\beta} \right), \quad (\text{S59})$$

where c electrons with spin $\alpha \in \{\uparrow, \downarrow\} \equiv \{1, 2\}$ coexist with local moments $\mathbf{S}_{i\mu}$ distributed over a checkerboard lattice. The hopping amplitudes are defined such that $t_{i\mu, j\nu} = t_1$ (t_2) on the solid (dashed) bonds of the lattice shown in Fig. 1(a) of the main paper. Furthermore, $\boldsymbol{\sigma} = (\sigma^x, \sigma^y, \sigma^z)$ is a vector of Pauli matrices.

Replacing the local-moment operators by their classical expectation values $\pm S$ in a two-sublattice Néel state yields a purely electronic Hamiltonian which describes the motion of electrons in a staggered field. It is spin-diagonal and can be written as

$$\mathcal{H}_K = \sum_{\mathbf{k}\alpha} \begin{pmatrix} c_{\mathbf{k}A\alpha}^\dagger & c_{\mathbf{k}B\alpha}^\dagger \end{pmatrix} \begin{pmatrix} -2t_2 \cos(k_x + k_y) + \frac{(-1)^\alpha K}{4} & -4t_1 \gamma_{\mathbf{k}} \\ -4t_1 \gamma_{\mathbf{k}} & -2t_2 \cos(k_x - k_y) - \frac{(-1)^\alpha K}{4} \end{pmatrix} \begin{pmatrix} c_{\mathbf{k}A\alpha} \\ c_{\mathbf{k}B\alpha} \end{pmatrix}. \quad (\text{S60})$$

Diagonalizing the 2×2 matrix yields the spectrum in Eq. (9) of the main text.

B. SU(3) hexatriangular Kondo-lattice model

As noted in the main text, the proper generalization of Eq. (S59) to a system with SU(3) symmetry is given by [6]

$$\mathcal{H}_K = - \sum_{i\mu, j\nu} \left(t_{i\mu, j\nu} c_{i\mu\alpha}^\dagger c_{j\nu\alpha} + \text{h.c.} \right) - \frac{K}{2M} \sum_{i\mu} \sum_{n=1}^8 S_{i\mu}^n \left(c_{i\mu\alpha}^\dagger \lambda_{\alpha\beta}^n c_{i\mu\beta} \right), \quad (\text{S61})$$

where $\alpha, \beta \in \{1, 2, 3\} \equiv \{A, B, C\}$ are flavor indices, n labels the independent generators of the SU(3) algebra, and λ^n denote the Gell-Mann matrices. Following standard notation, we associate the two diagonal generators of SU(3) with $n=3$ and $n=8$. In contrast, the $S_{i\mu}^n$ operators consist of a $(M, 0)$ irreducible representation of the generators of SU(3), which are related to the nine operators $S_{i\mu}^{\alpha\beta}$ introduced in Section S2 via Eq. (S21).

Proceeding as in Section S3A, we study the Hamiltonian (S61) within a semiclassical approximation for the local moments, in which we replace the operators $S_{i\mu}^n$ by their expectation value with respect to the three-color product state $|\psi\rangle$. Explicitly,

$$S_{i\mu}^n \rightarrow \langle \psi | S_{i\mu}^n | \psi \rangle = \langle \mu | S_{i\mu}^n | \mu \rangle = \frac{M}{2} (\delta_{n3} + \delta_{n8}) \lambda_{\mu\mu}^n. \quad (\text{S62})$$

The now purely electronic Hamiltonian becomes

$$\begin{aligned} \mathcal{H}_K^{\text{MF}} &= -t_1 \sum_{j, \delta_1} \left(c_{j\alpha}^\dagger c_{j+\delta_1, \alpha} + \text{h.c.} \right) - t_2 \sum_{j, \delta_{2\mu}} \left(c_{j\alpha}^\dagger c_{j+\delta_{2\mu}, \alpha} + \text{h.c.} \right) - \frac{K}{4} \sum_{i\mu} (\lambda_{\mu\mu}^3 \lambda_{\alpha\beta}^3 + \lambda_{\mu\mu}^8 \lambda_{\alpha\beta}^8) c_{i\mu\alpha}^\dagger c_{i\mu\beta} \\ &= -t_1 \sum_{\mathbf{k}\mu} \left[\left(\sum_{\delta_1} e^{i\mathbf{k} \cdot \delta_1} \right) c_{\mathbf{k}\mu\alpha}^\dagger c_{\mathbf{k}, \mu+1, \alpha} + \text{h.c.} \right] - 2t_2 \sum_{\mathbf{k}\mu} \cos(\mathbf{k} \cdot \delta_{2\mu}) c_{\mathbf{k}\mu\alpha}^\dagger c_{\mathbf{k}\mu\alpha} - K \sum_{\mathbf{k}\mu} \Lambda_{\mu\alpha} c_{\mathbf{k}\mu\alpha}^\dagger c_{\mathbf{k}\mu\alpha}. \end{aligned} \quad (\text{S63})$$

Here, the sets of vectors $\{\delta_1\}$ and $\{\delta_{2\mu}\}$ are the same as those specified in Eqs. (S26) and (S27), while the matrix

$$\Lambda = \frac{1}{6} \begin{pmatrix} 2 & -1 & -1 \\ -1 & 2 & -1 \\ -1 & -1 & 2 \end{pmatrix}. \quad (\text{S64})$$

As in the $SU(2)$ case, Eq. (S63) is diagonal in the flavor index α and splits into three 3×3 blocks $\mathcal{H} = \sum_{\mathbf{k}\alpha} \Psi_{\mathbf{k}\alpha}^\dagger \mathbb{M}_{\mathbf{k}\alpha} \Psi_{\mathbf{k}\alpha}$, with $\Psi_{\mathbf{k}\alpha} = (c_{\mathbf{k}A\alpha} \ c_{\mathbf{k}B\alpha} \ c_{\mathbf{k}C\alpha})^\top$ and

$$\mathbb{M}_{\mathbf{k}\alpha} = - \begin{pmatrix} 2t_2 \cos(\mathbf{k} \cdot \boldsymbol{\delta}_{2A}) + K\Lambda_{A\alpha} & 3t_1 \tilde{\gamma}_{\mathbf{k}} & 3t_1 \tilde{\gamma}_{\mathbf{k}}^* \\ 3t_1 \tilde{\gamma}_{\mathbf{k}}^* & 2t_2 \cos(\mathbf{k} \cdot \boldsymbol{\delta}_{2B}) + K\Lambda_{B\alpha} & 3t_1 \tilde{\gamma}_{\mathbf{k}} \\ 3t_1 \tilde{\gamma}_{\mathbf{k}} & 3t_1 \tilde{\gamma}_{\mathbf{k}}^* & 2t_2 \cos(\mathbf{k} \cdot \boldsymbol{\delta}_{2C}) + K\Lambda_{C\alpha} \end{pmatrix}. \quad (\text{S65})$$

To obtain the “electronic” spectrum, we diagonalize the three matrices $\mathbb{M}_{\mathbf{k}\alpha}$ numerically. The result is in Fig. 3(b) of the main paper.

C. Symmetries of the $SU(3)$ electronic bands

If $s_{i\mu}^n = c_{i\mu\alpha}^\dagger \tau_{\alpha\beta}^n c_{i\mu\beta}$ denotes the local flavor density of c fermions, then the properties

$$\left[c_{i\mu\alpha}^\dagger c_{j\nu\alpha}, s_{i\mu}^n + s_{j\nu}^n \right] = 0, \quad \left[\sum_{n=1}^8 S_{i\mu}^n s_{i\mu}^n, S_{i\mu}^n + s_{i\mu}^n \right] = 0, \quad (\text{S66})$$

imply that the Hamiltonian (S61) is invariant under global $SU(3)$ transformations acting identically on S and s operators:

$$\left[\mathcal{H}_K, \prod_{i\mu} e^{-i(S_{i\mu}^n + s_{i\mu}^n)\theta_n} \right] = 0. \quad (\text{S67})$$

If we additionally use the fact that the S degrees of freedom order in a three-color state, which is invariant under $SU(3)$ transformations generated by S^3 and S^8 , then we find that

$$\left[\mathcal{H}_K^{\text{MF}}, \prod_{i\mu} e^{-is_{i\mu}^3 \theta_3} \right] = \left[\mathcal{H}_K^{\text{MF}}, \prod_{i\mu} e^{-is_{i\mu}^8 \theta_8} \right] = 0. \quad (\text{S68})$$

This explains why the fermionic flavor is a good quantum number, as we observed in the explicit calculations above. Note, however, that $\left[\mathcal{H}_K^{\text{MF}}, \prod_{i\mu} e^{-is_{i\mu}^n \theta_n} \right] \neq 0$ for $n \notin \{3, 8\}$, since the mean-field Hamiltonian assumes that $SU(3)$ symmetry is spontaneously broken in the S sector.

The symmetries of the band structure are again dictated by the spin point group in Eq. (S52). For instance, the symmetry $T_A = [(BC) || M_A]$ enforces the degeneracy of B (green) and C (red) bands along the line $k_x = 0$ and the vertical boundaries of the Brillouin zone, which are formed by momenta that satisfy $M_A \mathbf{k} = \mathbf{k} + \mathbf{G}$ for a reciprocal lattice vector \mathbf{G} . Similar considerations, paired with the fact that the bands are inversion-symmetric, yield all of the crossings observed in Fig. 3(c,d) of the main text between bands of different colors.

-
- [1] T. A. Tóth, A. M. Läuchli, F. Mila, and K. Penc, Phys. Rev. Lett. **105**, 265301 (2010).
 - [2] B. Bauer, P. Corboz, A. M. Läuchli, L. Messio, K. Penc, M. Troyer, and F. Mila, Phys. Rev. B **85**, 125116 (2012).
 - [3] A. Läuchli, F. Mila, and K. Penc, Phys. Rev. Lett. **97**, 087205 (2006).
 - [4] H. Tsunetsugu and M. Arikawa, J. Phys. Soc. Jpn. **75**, 083701 (2006).
 - [5] A. Zee, *Group Theory in a Nutshell for Physicists*, Princeton University Press (2016).
 - [6] O. Parcollet, A. Georges, G. Kotliar, and A. Sengupta, Phys. Rev. B **58**, 3794 (1998).
 - [7] D. M. Litvin and W. Opechowski, Physica **76**, 538 (1974).
 - [8] D. M. Litvin, Acta Cryst. **A33**, 279 (1977).